

**A THESIS REPORT**  
**ON**  
**MODELLING AND ANALYSIS OF WEAR FOR VAPOUR**  
**DEPOSITION COATINGS**  
**SUBMITTED IN PARTIAL FULFILLMENT OF THE REQUIREMENTS FOR THE**  
**AWARD OF THE DEGREE OF**  
**MASTER OF TECHNOLOGY**  
**IN**  
**PRODUCTION AND INDUSTRIAL ENGINEERING**

**SUBMITTED BY**

**MOHIT KATARIA**  
**2K13/PIE/12**

**UNDER THE SUPERVISION OF**

**Dr. QASIM MURTAZA**  
**ASSOCIATE PROFESSOR**

**Mr. SHAILESH MANI PANDEY**  
**ASSISTANT PROFESSOR**



**DEPARTMENT OF MECHANICAL ENGINEERING**  
**DELHI TECHNOLOGICAL UNIVERSITY, DELHI**  
**INDIA**

**JUNE 2015**

## **DECLARATION**

I hereby declare that the work presented in this report, titled “**MODELLING AND ANALYSIS OF WEAR FOR VAPOUR DEPOSITION COATINGS**”, in partial fulfilment for the award of the degree of M.Tech in production and industrial engineering, submitted in the Department of mechanical engineering, Delhi Technological University, Delhi, is original and to the best of my knowledge and belief, it has not been submitted in part or full for the award of any other degree or diploma of any other university or institute, except where due acknowledgement has been made in the text.

Mohit Kataria

Roll No. 2K13/PIE/12

M.Tech. production and industrial engineering

Date:

## **CERTIFICATE**

This is to certify that the research work embodied in this dissertation entitled **“MODELLING AND ANALYSIS OF WEAR FOR VAPOUR DEPOSITION COATINGS”**. Submitted by Mohit Kataria, Roll no. 2K13/PIE/12 student of Master of Technology in production and industrial engineering under Department of Mechanical Engineering, Delhi Technological University, Delhi is a bonafide record of the candidate’s own work carried out by him under my guidance. This work is original and has not been submitted in part or full for award of any other degree or diploma to any university or institute.

(Dr. QASIM MURTAZA )

Associate Professor

Department of Mechanical Engineering

Delhi Technological University, Delhi,

India

(Mr. Shailesh Mani Pandey)

Assistant Professor

Department of Mechanical Engineering

Delhi Technological University, Delhi,

India

Date:

## **ACKNOWLEDGEMENT**

I express my deepest gratitude to my guide Dr. Qasim Murtaza, Associate Professor & Mr. Shailesh Mani Pandey, Assistant Professor Department of Mechanical Engineering, Delhi Technological University, whose encouragement, guidance and support from the initial to the final level enabled me to develop an understanding of the subject. His suggestions and ways of summarizing the things made me go for independent studying and trying my best to get the maximum in my topic, this made my circle of knowledge very vast. I am highly thankful to him for guiding me in this project.

I am also grateful to Dr. R.S. Mishra, professor HOD, Mechanical Engineering Department, DTU for his immense support.

Finally, I take this opportunity to extend my deep appreciation to my family, for their endless support during the crucial times of the completion of my project.

Mohit Kataria

Roll No. 2K13/PIE/12

M.Tech. Production And Industrial Engineering

# TABLE OF CONTENTS

<b>CERTIFICATE.....</b>	<b>2</b>
<b>ACKNOWLEDGEMENT.....</b>	<b>3</b>
<b>LIST OF FIGURES .....</b>	<b>7</b>
<b>LIST OF TABLES .....</b>	<b>9</b>
<b>Chapter 1 Introduction.....</b>	<b>10</b>
1.0 Surface Engineering.....	10
1.1 Coatings.....	12
1.1.1 Chromium Electroplating.....	13
1.2 Safety and Environment Concerns.....	13
1.3 Coating Material.....	14
1.4 Wear Resistant Coatings and its Classification.....	16
1.5 Vacuum Dependent Coating Techniques.....	19
1.5.1 Physical Vapour Deposition.....	20
1.5.1.1 Evaporation.....	21
1.5.1.2 Ion Plating.....	22
1.5.1.3 Sputtering.....	23
1.5.2 Chemical Vapour Deposition.....	24
1.5.3 Ion Implantation.....	25
1.6 Types of Wear in the Coating.....	26
1.6.1 Adhesive Wear.....	27
1.6.1.1 Metal Transfer Mechanism.....	28
1.6.2 Fatigue Wear.....	29
1.6.3 Fretting Wear.....	30

1.6.3.1 Effect of Temperature on Fretting.....	30
1.6.4 Diffusive Wear.....	31
1.6.5 Impact Wear.....	31
1.6.6 Cavitation Wear.....	32
1.6.7 Erosive Wear.....	32
1.6.7.1 Mechanism of Erosive Wear.....	33
1.6.8 Abrasive Wear.....	33
1.6.8.1 Mechanism of Abrasive Wear.....	34
<b>Chapter 2 Literature Review.....</b>	<b>36</b>
<b>Chapter 3 Modelling of Wear.....</b>	<b>41</b>
3.1 The Integrated Wear Model.....	43
3.2 The Transient Wear.....	44
3.3 Steady State Wear.....	44
3.3.1 Standard Wear Coefficient.....	44
3.3.2 Net Steady State Wear Coefficient.....	45
3.4 Transient Distance.....	45
3.5 Second Wear Coefficient.....	46
3.6 Effect of Exponential Factor.....	47
<b>Chapter 4 Result and Discussion.....</b>	<b>48</b>
4.0 Load vs. Volume Loss.....	48
4.1 Standard Wear Coefficient vs. Volume Loss.....	50
4.2 Load vs. Average Standard Wear Coefficient.....	56
4.3 Conclusion.....	59
REFERENCES.....	60

## ABSTRACT

Wear takes place where any two contacting rubbing surfaces found. To prevent wear Coatings on the surface are deposited. In this study an attempt is made to find out the standard wear (dimensionless constant) coefficient which is a very crucial factor decides the amount of volume loss for particular contacting surfaces under a given load, sliding distance and sliding velocity as proposed by Archard. On pin on disc apparatus test is performed to find out the volume loss for Cast iron and chromium nitride coating with load (50, 60,70,80,90,100 N) at sliding velocities (1, 2, 3m/s) for a constant sliding distance of 2500m. Variation of standard wear coefficient with volume loss is represented at different sliding velocities for both Cast iron and chromium nitride coating. The results show a decreasing trend for standard wear coefficient with volume loss when load is kept increasing and sliding velocities are kept constant at 1m/s, 2m/s, 3m/s. It shows a good agreement with the model as the ratio of volume/load decreases thereby decreasing the standard wear coefficient. An average standard wear coefficient value is obtained by taking the average of standard coefficient values at different velocities. Plot between average standard coefficient and load shows a decreasing trend which is a good agreement with the model.

## LIST OF FIGURES

FIGURE 1.1 COATING DEPOSITION TECHNIQUES	17
FIGURE 1.2 CLASSIFICATION OF PVD	19
FIGURE 1.3 SCHEMATIC DIAGRAM OF EVAPORATION PROCESS	21
FIGURE 1.4 SCHEMATIC DIAGRAM OF THE ION PLATING PROCESS	22
FIGURE 1.5 SCHEMATIC DIAGRAM OF THE SPUTTERING PROCESS	23
FIGURE 1.6 SCHEMATIC DIAGRAM OF THE CVD PROCESS	24
FIGURE 1.7 SCHEMATIC DIAGRAM OF THE ION IMPLANTATION PROCESS	25
FIGURE 1.8 SCHEMATIC DIAGRAM OF THE FORMATION OF AN ADHESIVE TRANSFER PARTICLE	27
FIGURE 1.9 FORMATION AND REMOVAL OF THE TRANSFER PARTICLE	28
FIGURE 1.10 SCHEMATIC ILLUSTRATIONS OF THE MECHANISMS OF IMPACT WEAR	31
FIGURE 1.11 TWO AND THREE BODY MODES OF ABRASIVE WEAR	34
FIGURE 3.1(A) WEAR VOLUME VERSUS SLIDING DISTANCE	41
FIGURE 3.1(B) STANDARD WEAR COEFFICIENT VERSUS SLIDING DISTANCE	41
FIGURE 3.2 THE INTEGRATED WEAR MODEL	42
FIGURE 4.1 VOLUME LOSS VS. LOAD FOR DIFFERENT SLIDING VELOCITIES FOR CAST IRON	48



FIGURE 4.2 VOLUME LOSS VS. LOAD FOR DIFFERENT SLIDING VELOCITIES FOR CHROMIUM	49
FIGURE 4.3 STANDARD WEAR COEFFICIENT VS. VOLUME LOSS FOR CAST IRON AT 1 M/S	50
FIGURE 4.4 STANDARD WEAR COEFFICIENT VS. VOLUME LOSS FOR CHROMIUM NITRIDE AT 1 M/S	51
FIGURE 4.5 STANDARD WEAR COEFFICIENT VS. VOLUME LOSS FOR CAST IRON AT 2M/S	52
FIGURE 4.6 STANDARD WEAR COEFFICIENT VS. VOLUME LOSS FOR CHROMIUM NITRIDE AT 2M/S	53
FIGURE 4.7 STANDARD WEAR COEFFICIENT VS. VOLUME LOSS FOR CAST IRON AT 3M/S	54
FIGURE 4.8 STANDARD WEAR COEFFICIENT VS. VOLUME LOSS FOR CHROMIUM NITRIDE AT 3M/S	55
FIGURE 4.9 LOAD VS. STANDARD WEAR COEFFICIENT FOR CAST IRON	56
FIGURE 4.10 LOAD VS. STANDARD WEAR COEFFICIENT FOR CHROMIUM NITRIDE COATING	57

## LIST OF TABLES

TABLE 1.1 : SOME PROCESSES FOR SURFACE ENGINEERING	11
TABLE 1.2: AVAILABLE TECHNIQUES TO IMPROVE TRIBOLOGICAL CHARACTERISTICS	17
TABLE 4.1: FOR CAST IRON	48
TABLE 4.2: FOR CHROMIUM NITRIDE COATING	49
TABLE 4.3: FOR CAST IRON AT SLIDING VELOCITY 1M/S	50
TABLE 4.4: FOR CHROMIUM NITRIDE COATING AT SLIDING VELOCITY 1M/S	51
TABLE 4.5: FOR CAST IRON AT SLIDING VELOCITY 2M/S	52
TABLE 4.6: FOR CHROMIUM NITRIDE COATING AT SLINDING VELOCITY 2M/S	53
TABLE 4.7: FOR CAST IRON AT SLIDING VELOCITY 3M/S	54
TABLE 4.8: FOR CHROMIUM NITRIDE COATING AT SLIDING VELOCITY 3M/S	55
TABLE 4.9: LOAD VS. STANDARD WEAR COEFFICIENT FOR CAST IRON	56
TABLE 4.10: LOAD VS. STANDARD WEAR COEFFICIENT FOR CHROMIUM NITRIDE COATING	57

## INTRODUCTION

### 1.0 SURFACE ENGINEERING

It is the process of changing properties of the surface and the region surrounding the surface. Wear and friction together with lubrication form the scientific discipline called Tribology. There are so many processes used for surface engineering. Some of them are listed below in Table 1.1. Each process has its advantages, disadvantages, and applications. In some cases surface modification processes can be used to modify the substrate surface prior to depositing a film or coating. For example, a steel surface can be hardened by plasma nitriding prior to the deposition of a hard coating by a physical vapor deposition (PVD) process. In other cases, a surface modification process can be used to change the properties of an overlay coating. For example, a sputter-deposited coating on an aircraft turbine blade can be shot peened to densify the coating and place it into compressive stress. An atomistic deposition process is one in which the overlay material is deposited atom-by atom. The resulting film can range from single crystal to amorphous, fully dense to less than fully dense, pure to impure, and thin to thick. Generally the term “thin film” is applied to layers which have thicknesses on the order of a micron or less (1 micron =  $10^{-6}$  meters) and may be as thin as a few atomic layers. Thicker deposits are called coatings. The term “thick film” is usually not used for thick atomistically deposited vacuum deposits as that term is used for “paint-on, fire-on” types of deposition. Often the properties of thin films are affected by the properties of the underlying material (substrate) and can vary through the thickness of the film. Thicker layers are generally called coatings. An atomistic deposition process can be done in a vacuum, gaseous, or electrolytic environment.

**Table 1.1: Some Processes for Surface Engineering.**

<b>Atomistic/Molecular Deposition</b>	<b>Bulk Coatings</b>
<i>Electrolytic Environment</i>	<i>Wetting Processes</i>
Electroplating	Dip coating
Electro less plating	Spin coating
Displacement plating	Painting
Electrophoretic deposition	<i>Fusion Coatings</i>
<i>Vacuum Environment</i>	Thick films
Vacuum evaporation	Enameling
Ion beam sputter deposition	Sol-gel coatings
Ion beam assisted deposition (IBAD)	Powder coating
Laser vaporization	<i>Solid Coating</i>
Hot-wire and low pressure CVD	Cladding
Jet vapor deposition	Weld overlay
<i>Plasma Environment</i>	Gilding
Sputter deposition	<b><i>Surface Modification</i></b>
Arc vaporization	<i>Chemical Conversion</i>
Ion plating	Wet chemical solution (dispersion & layered)
Plasma enhanced (PE) CVD	Gaseous (thermal) plasma
Plasma polymerization	<i>Electrolytic Environment</i>
<i>Chemical Vapor Environment</i>	Anodizing
Chemical vapor deposition (CVD)	Ion substitution
Pack cementation	Plasma electrolysis
<i>Chemical Solution</i>	<i>Mechanical</i>
Spray pyrolysis	Shot peening
Chemical reduction	Work hardening
<b><i>Particulate Deposition</i></b>	<i>Thermal Treatment</i>
<i>Thermal Spray</i>	Thermal stressing
Flame spray	<i>Ion Implantation</i>
Arc-wire spray	Ion beam
Plasma spraying	Plasma immersion ion implantation (PIII)
D-gun	<i>Roughening and Smoothing</i>

High-velocity-oxygen-fuel (HVOF)	Chemical
<i>Impact Plating</i>	Mechanical
Mechanical plating	Chemical–mechanical polishing
	Sputter texturing
	<i>Enrichment and Depletion</i>
	Thermal
	Chemical

## 1.1 COATINGS

Materials are the rare resources of the earth and it is very important to protect them for efficient and proper use. There are various surface treating phenomena to improve the tribo-mechanical properties of materials. Surface coating is also a phenomenon to form a protective layer on the top of material or a brittle, wear resistant material can be improved by the support of a more ductile bulk material. It is also possible to combine several material properties within coating like a hard phase with a lubricious phase.

The hard phase is usually a carbide or nitride and the lubricious phase is often amorphous carbon (a-C) that can reduce adhesion and sticking to the counter surface. There are several deposition techniques low-friction wear resistant properties frequently used in various machine elements to reduce energy losses and some specific properties which are needed can be attained by surface coating phenomenon.

Physical vapour deposition (PVD) is a common technique for thin coatings in range of 1-10µm and also offered high quality of coating at relatively low substrate temperature with variable composition. PVD can be achieved by either evaporation or sputtering of a solid source in vacuum. In both cases, the vapour can form a coating either with the same composition as the evaporated material or in an altered form after reaction with a gas introduced into the deposition chamber (such as TiN formed from sputtered Ti reacted with N<sub>2</sub> gas).

The superior coating properties are achieved due to a multi-layer microstructure and a special coating composition that contains carbon, deposited in diamond-like form, as well as hydrogen

and tungsten. The unique structure can be produced for a coating thickness of 10 microns, more than three times that of the industry's latest DLC coating. A specialized advanced process based on the combination of physical vapour deposition and plasma-assisted chemical vapour deposition, specifically developed for piston ring application, is used in applying Carbo-Glide. The coating's multi-layer architecture, together with the company's surface machining and finishing expertise, ensure the integrity of the coating structure, optimal adhesion of the coating and high coating stability on both steel and cast iron rings [2].

### **1.1.1 Chromium Electroplating**

Hard chromium coatings are used in several fields. Due to the low friction of hard chromium coatings they are used in applications like cylinders, engine valves, shafts and bearings. Chrome coating has been used since 1940's is a very hard and common coating. In starting chromium coating was very popular hard and common coating due to cheap, wear and corrosion resistance. Further it moves towards electroplating of chromium which is replaced by chromium nitride coating due to environmental issues concerned with hexavalent chromium( $\text{Cr}^{+6}$ ). This was very hazardous so it has to be removed from environment and waste water after plating. Thickness is a critical parameter in CrN coating by PVD it affects by the supply pressure of nitrogen and other parameters also. Various Tribo-mechanical properties like wear friction and hardness affects by the coating thickness. Chrome plating was declared unfriendly to the environment the U.S. *Environmental Protection Agency* (EPA) same year the European Union directive *Restriction of Hazardous Substances* (RoHS) decided to ban hexavalent chrome.

## **1.2 SAFETY AND ENVIRONMENTAL CONCERNS**

Safety and environmental concerns are areas where there is a great deal of difference between the development and manufacturing environments. This may be due to the types or amounts of materials used. For example, a common drying agent is anhydrous alcohol, which can be used safely in a well-ventilated open area by careful people. However, in manufacturing, fire regulations do not allow alcohol to be used in the open environment because of its low flash point and large volume. Instead, the alcohol vapor must be contained and condensed or some other drying technique must be used.

By US law, every worker must be informed about the potential dangers of the chemicals that they encounter in the workplace (OSHA – Hazard Communication Standard 29 CFR 1910.1200). This includes common chemicals, such as household dishwasher soaps. It is the responsibility of managers to keep workers informed about the chemicals being used and their potential hazards. Chemical manufacturers must provide users with MSDSs on all their chemicals. These MSDSs must be made available to all workers. There are MSDSs on all kinds of chemical, ranging from the toner used in copiers, to common household detergents, to really hazardous chemicals such as hydrofluoric acid (HF). Information on environmental aspects of processing can be obtained from the Centre for Environmental Research Information.

### **1.3 COATING MATERIAL**

Coating material is chosen to meet the demands of application and it should be resistant to damage in emergency conditions. For Ex-In piston rings according to running condition at various load and sliding velocity for a long run. Elasticity and corrosion resistance of the ring material is required. The ring coating, if applied, needs to work well together with both the ring and the liner materials, as well as with the lubricant. As one task of the rings is to conduct heat to the liner wall, good thermal conductivity is required. Grey cast iron is used as the main material for piston rings. From a tribological point of view, the grey cast iron is beneficial, as a dry lubrication effect of the graphite phase of the material can occur under conditions of oil starvation. Furthermore, the graphite phase can act as an oil reservoir that supplies oil at dry starts or similar conditions of oil starvation. Reduced width piston rings in gasoline engines to match reductions in the overall height of pistons, and increasing combustion pressures in diesel engines call for materials with increased strength characteristics. These challenges are met by the use of high-chromium alloyed steels and spring steels. The greater durability under increased stresses is demonstrated by the improved fatigue strength manifested as form stability.

Some materials deposited by PVD processes are as follows:

- Gold – electrical conductor, anticorrosion surface, infrared (IR) reflectance
- Silver – electrical conductor, heat reflector, optical mirrors, low shear film lubricant
- Aluminium – electrical conductor, optical reflectance, corrosion resistance
- Copper – electrical conductor, solder ability

- Cadmium – corrosion resistance (being phased out)
- Zinc – corrosion resistance
- Titanium – “glue layer” to oxides
- Chromium – “glue layer” to oxides, corrosion resistance, hard coating
- Palladium – galvanic corrosion layer between Ti and Au
- Molybdenum – “glue layer” to oxides
- Tantalum – corrosion and erosion resistance
- Beryllium – freestanding X-ray windows
- Carbon (DLC) – hard coat, chemically resistant, low friction
- Nickel – “glue layer” to metals, basecoat on brass
- Silicon – semiconductor devices
- Selenium – photosensitive material

Some mixtures (physical mixtures or above solubility limits):

- Silicon + dopants – semiconductor devices
- Nano phase composites – hard coatings

Some glasses:

- Amorphous silicon (a-Si) – semiconductor, photovoltaic
- Phosphorus + silicon oxides (PSGs) – encapsulant

Some alloys:

- Zinc + aluminium – corrosion protection
- Aluminium + copper + silicon – semiconductor metallization
- Indium + tin/oxide – transparent electrical conductor, IR reflection
- Nickel + chromium – “glue layer” to oxides, electrical resistance
- Tungsten + titanium – semiconductor metallization, diffusion barrier  
(W: Ti [90:10 wt%; 70:30 at %])

Some compounds:

- Titanium nitride – diffusion barrier coating, tool coating, decorative coating
- Titanium/Carbon nitride – tool coating, decorative coating
- Titanium/Aluminium nitride – wear coating
- Chromium nitride – hard coating, low friction
- Aluminium oxide – permeation barrier, diffusion barrier



- Titanium oxide – high index optical coating
- Silicon dioxide – low index optical coating
- Magnesium fluoride – low index optical coating
- Molybdenum di-sulphide – solid film lubricant
- Molybdenum di-selenide – solid film lubricant (electrical conductor)
- Tantalum oxide – high index optical coating
- Zinc sulphide – high index optical coating

Some layered systems:

- Ti/Au, Ti/Pd/Cu/Au, Ti/Ag, Ti/Pd/Ag – electrical conductor electrodes on oxides
- Cr/Au, Cr/Pd/Au – oxide metallization
- Mo/Au – oxide metallization
- TiN/Al – silicon metallization
- Ni/Cr – basecoat on brass
- Nano layered composites – hard/wear coatings
- ZnO<sub>x</sub>: Ag : Zn (thin): ZnO<sub>x</sub>: TiO<sub>x</sub>– low-e (low emission) glass coating
- SnO<sub>x</sub>: Ag : NiCr (thin) : SnO<sub>x</sub>– low-e glass coating on glass

## 1.4 WEAR RESISTANT COATINGS& ITS CLASSIFICATION

Tribo – mechanical properties of uncoated material can be improved by the coating of hard material to protect against wear. Abrasive wear, fretting wear and adhesive wear are often reduced by hard coating. Wear and friction is a critical problem in most of the application another benefit of hard chrome plating is that a cheap substrate material wear performance can be improved by coating of an exotic, high-performance material. Applications of wear resistant coatings are found in every industry, and for example, include mining excavator shovels and crushers. There are various methods for improving the wear properties of metal substrate some of them which are newly developed are very efficient to deposit a wear resistant coating. Localized heat treatment like thermal hardening and alloying some element like nitriding and carburizing are used to improve the wear resistance. Many of these methods have been in use for many years but unfortunately suffer from the disadvantage that the substrate needs to be heated to a high temperature. Carburizing, nitriding and carbonitriding in particular suffer from this problem. Most engineering items are made of steel and it is often found that some material other

than steel is needed to fulfill the wear and friction requirements. Many wear resistant materials are brittle or expensive and can only be used as a coating, so improved coating technology has extended the control of wear to many previously unprotected engineering components. Various coating techniques available with their principal merits and demerits are listed in Table 1.2.

**Table 1.2: Available techniques to improve its tribological Characteristics**

<b>Techniques</b>	<b>Principal Merits And Demerits</b>
PVD & CVD	Thin discrete coating; no limitations on materials
Thermal spraying	Very thick coatings possible but control of coating purity is difficult
Ion implantation	Thin diffuse coating; mixing with substrate inevitable
Laser glazing	Thick coatings; coating material must be able to melt
Friction surfacing	Simple technology but limited to planar surfaces; produces thick metal coating
Electroplating	Wide range of coating thicknesses, but adhesion to substrate is poor and only certain materials can be coated by this technique
Surface welding	Suitable for very thick coatings only; limited to materials stable at high temperatures; coated surfaces may need further preparation
Explosive cladding	Rapid coating of large areas possible and bonding to substrate is good. Can give a tougher and thicker coating than many other method

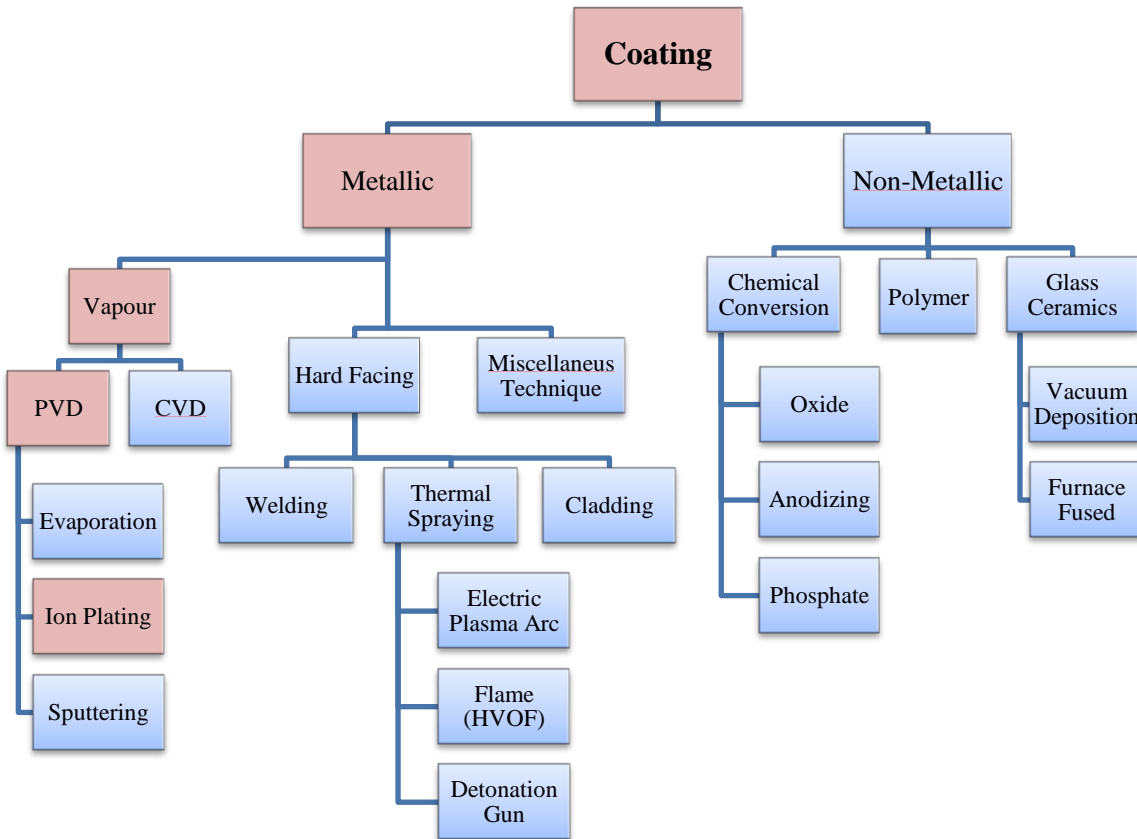


Figure 1.1 depicts the flow chart of various coating techniques. In which physical vapour deposition (PVD) and its types are discussed latter broadly. Thermal spray coating is also very popular according to industrial application among researchers. Cold spraying which is also a type of thermal spray is currently in trend due to its advantages. Some Non-metallic and nano-composite coating is also developed as per need in medical surgery equipment. Plasma assisted diffusion technologies are able to modify metallic surface by incorporation of light element like nitrogen, boron, and oxygen, such engineering techniques are widely used in automotive industry like piston rings coating.

## 1.5 VACUUM DEPENDENT COATING TECHNIQUES

Basic type of coating technique physical vapour deposition (PVD), chemical vapour deposition (CVD) and ion implantation are in current use. These are also suitable for precision components and thin coating of the range from 0.1-10 $\mu$ m. Process requires enclosure in a vacuum from which atmospheric oxygen and water have been removed. Removing of air from enclosure has some advantage over coating in air. The exclusion of contaminants results in strong adhesion between the applied coating and substrate and greatly improves the durability of the coating. Some high quality coating is also produced by plasma based process without any limitation on the coating or substrate material. Some of the most utilized applications of thin film deposition processes include:

- Single and multilayer films and coatings
- Nano-layered & Nano-composite materials
- Optical films for transmission and reflection
- Decorative films
- Decorative and wear-resistant (decorative/functional) coatings
- Corrosion-resistant films
- Electrically insulating layers for microelectronics
- Coating of engine turbine blades
- Coating of high strength steels to avoid hydrogen embrittlement
- Diffusion barrier layers for semiconductor metallization
- Magnetic films for recording media
- Transparent electrical conductors and antistatic coatings
- Wear and erosion-resistant (hard) coatings (tool coatings)
- Dry film lubricants
- Composite and phase-dispersed films and coatings
- Thin-walled freestanding structures and foils

### 1.5.1 Physical Vapour Deposition (PVD)

In physical vapour deposition coating is done by condensation in vacuum and glow discharge result a perfect adhesion between the atoms of coating material and the atoms of the substrate. Concerned to the materials metallic, intermetallic, ceramics or many other compound can be deposited onto the substrate by PVD. Porosity is also suppressed by the absence of dirt inclusions. In recent years, a number of specialized PVD techniques have been developed has its own advantages and range of preferred applications. Some applications of PVD range from the decorative to microelectronics, over a significant segment of the engineering, chemical, nuclear and related industries. Physical vapour deposition consists of three major techniques.

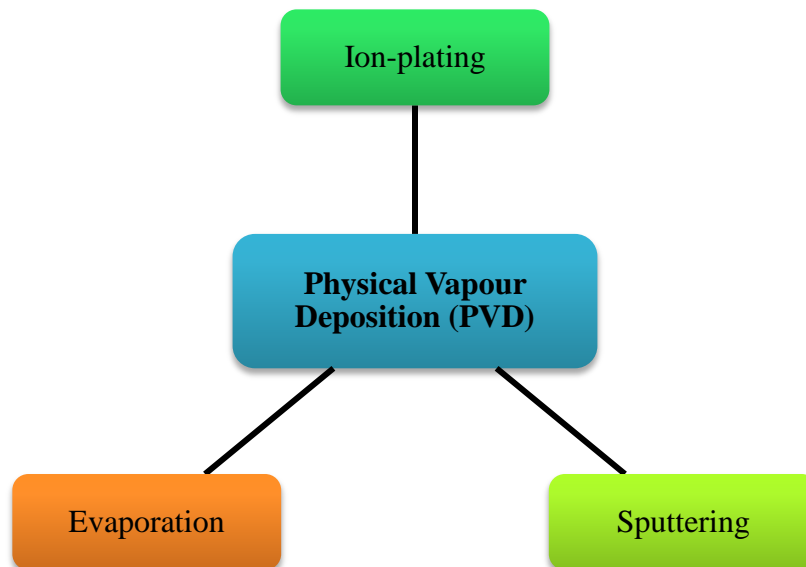


Figure 1.2: Classification of PVD

### **1.5.1.1 Evaporation**

It is also one of the relatively simple and cheap vacuum deposition processes for thickness of 1mm. Operating pressure and temperature range of evaporating coating material 10 – 6Pa and 1000 – 2000°C. At this pressure and temperature atoms travel in straight line towards substrate and condensation take place. For the proper bonding between the base plate and coated material kinetic energy of the source material atoms and the ambient gas atoms. To minimize these collisions the source to substrate distance is adjusted so that it is less than the free path of gas atoms. Because of the low kinetic energy of the vapour the coatings produced during the evaporation exhibit low adhesion and therefore are less desirable for tribological applications compared to other vacuum based deposition processes. Furthermore, because the atoms of vapour travel in straight lines to the substrate, this results in a ‘shadowing effect’ for surfaces which do not directly face the coating source and common engineering components such as spheres, gears, moulds and valve bodies are difficult to coat uniformly. The source material can be heated by electrical resistance, eddy currents, electron beam, laser beam or arc discharge. Electric resistance heating usually applies to metallic materials having a low melting point while materials with a high melting point, e.g. refractory materials, need higher power density methods, e.g. electron beam heating. Since the coating material is in the electrically neutral state it is expelled from the surface of the source. The substrate is also pre-heated to a temperature of about 200 – 1600°C.

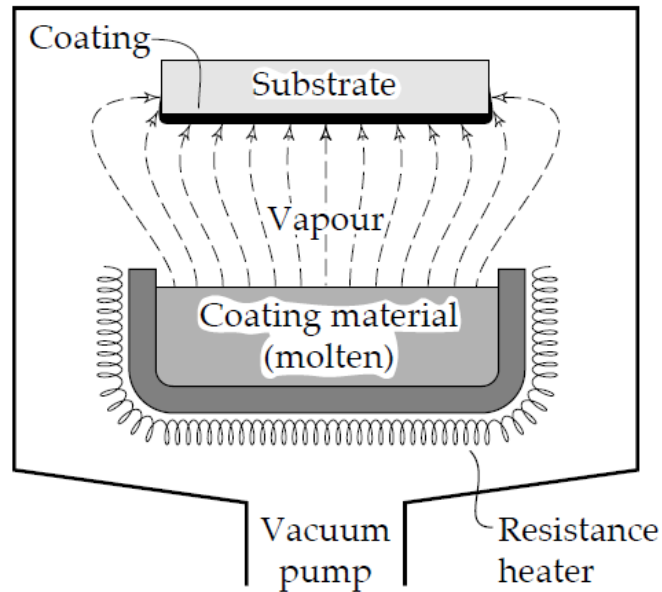


Figure 1.3: Schematic diagram of the evaporation process

### 1.5.1.2 Ion-plating

The process of ion-plating therefore involves thermal evaporation of the coating material in a manner similar to that used in the evaporation process and ionization of the vapour due to the presence of a strong electric field and previously ionized low pressure gas, usually argon. The argon and metal vapour ions are rapidly accelerated towards the substrate surface, impacting it with a considerable energy. Glow discharge utilized in these phenomena by applying electric potential applied between two electrodes immersed in gas at reduced pressure, a stable passage of current is possible. At a voltage coating material can be transferred from the 'source' electrode to the 'target' electrode which contains the substrate. Before to ion-plating, surface impurities of the base material need to be removed by high energy inert gas for better bonding. Ion plating processes can be classified into two general categories: glow discharge (plasma) ion plating conducted in a low vacuum of 0.5 to 10 Pa and ion beam ion plating (using an external ionization source) performed in a high vacuum of  $10^{-5}$  to  $10^{-2}$  Pa. The most important aspect of ion-plating which distinguishes this process from the others is the modification of the microstructure and composition of the deposit caused by ion bombardment [8]. The ion-plating process is schematically illustrated in Figure 1.4.

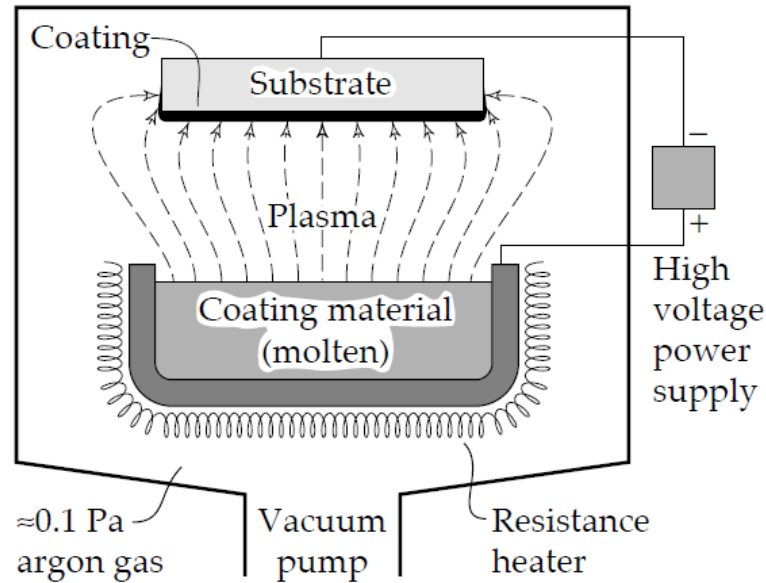


Figure 1.4: Schematic diagram of the ion-plating process

### 1.5.1.3 Sputtering

It based on dislodging and ejecting the atoms from the coating material by bombardment of high-energy ions of heavy inert or reactive gases, usually argon. Coating material is not evaporated and instead, ionized argon gas is used to dislodge individual atoms of the coating substance. For example, in glow-discharge sputtering a coating material is placed in a vacuum chamber which is evacuated to  $10^{-5}$  to  $10^{-3}$  Pa and then back-filled with a working gas, e.g. argon, to a pressure of 0.5 to 10 Pa. The substrate is positioned in front of the target so that it intercepts the flux of dislodged atoms. Therefore the coating material arrives at the substrate with far less energy than in ion-plating so that a distinct boundary between film and substrate is formed. When atoms reach the substrate, a process of very rapid condensation occurs. The condensation process is critical to coating quality and unless optimized by the appropriate selection of coating rate, argon gas pressure and bias voltage, it may result in a porous crystal structure with poor wear resistance. The most characteristic feature of the sputtering process is its universality. Since the coating material is transformed into the vapour phase by mechanical (momentum exchange) rather than a chemical or thermal process, virtually any material can be coated. Therefore the main advantage of sputtering is that substances which decompose at elevated temperatures can be sputtered and substrate heating during the coating process is usually negligible. Although ion-



plating produces an extremely well bonded film, it is limited to metals and thus compounds such as molybdenum disulphide which dissociate at high temperatures cannot be ion-plated. The sputtering process is schematically illustrated in Figure 1.5.

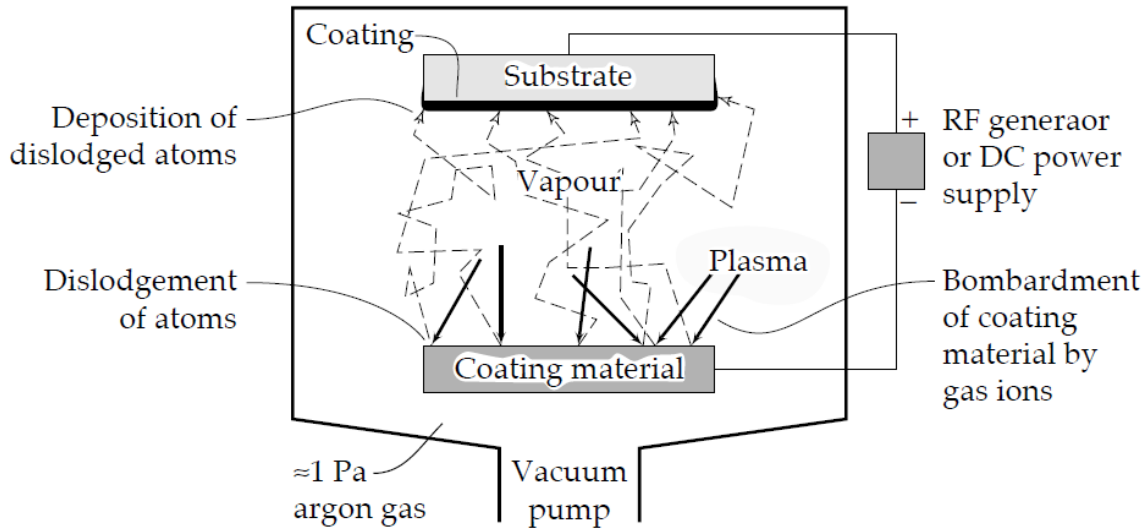


Figure 1.5: Schematic diagram of the sputtering process

### 1.5.2 Chemical Vapour Deposition (CVD)

Coating material will be formed in vapour state by volatilization if not already in vapour state further it is forced to flow by a pressure difference or action of carrier gas towards the substrate surface. To produce a metallic coating frequently reactant gases and other required material introduced like coating of titanium nitride with the help of introducing nitrogen during titanium evaporation. Temperature and pressure range 150 – 2200°C and 50 Pa for happening of chemical reaction at atmospheric pressure. Vapour will be condensing at relatively cool surface so all the parts of the system need to be hot as the vapour source. Generally, reaction portion of the system is more higher than vapour source but below the melting temperature of coating. Electric resistance and infra-red heating or inductance usually uses to heat the substrate. During the process the coating material is deposited, atom by atom, on the hot substrate. Although CVD coatings usually exhibit excellent adhesion, the requirements of high substrate temperature limit their applications to substrates which can withstand these high temperatures. The CVD process at

low pressure allows the deposition of coatings with superior quality and uniformity over a large substrate area at high deposition rates.

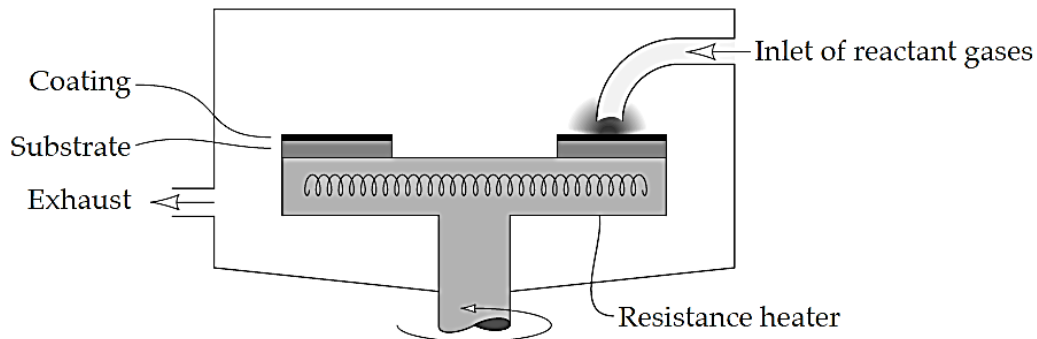


Figure 1.6: Schematic diagram of the CVD

### 1.5.3 Ion Implantation

The energy of ions in plasma can be raised to much higher levels than is achieved either in ion-plating or sputtering. If sufficient electrical potential is applied then the plasma can be converted to a directed beam which is aimed at the material to be coated allowing the controlled introduction of the coating material into the surface of the substrate. This process is known as ion implantation. During the process of ion implantation, ions of elements, e.g. nitrogen, carbon or boron, are propelled with high energy at the specimen surface and penetrate the surface of the substrate. It is done in a vacuum in the range of  $10^{-3}$  to  $10^{-4}$  Pa by means of high energy beams. The mass of implanted ions is limited by time, therefore compared to other surfaces; the layers of ion-implanted surfaces are very shallow, about 0.01 to 0.5  $\mu\text{m}$ . The thickness limitation of the implanted layer is the major disadvantage of this method. The coatings generated by ion implantation are only useful in lightly loaded contacts. The technique allows for the implantation of metallic and non-metallic coating materials into metals, cermets, ceramics or even polymers. The ion implantation is carried out at low temperatures. Despite the thinness of the modified layer, a long lasting reduction in friction and wear can be obtained, for example, when nitrogen is implanted into steel. The main advantage of the ion implantation process is that the treatment is very clean and the deposited layers very thin, hence the tolerances are maintained and the precision of the component is not distorted. Ion implantation is an expensive process since the cost of the equipment and running costs are high. The ion implantation process is schematically illustrated in Figure 1.7.

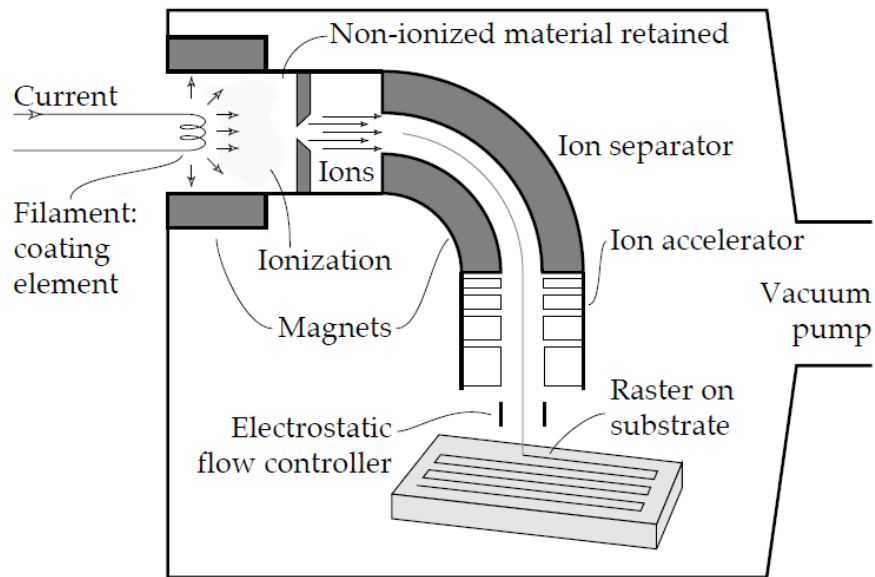


Figure 1.7: Schematic diagram of the ion implantation process

## 1.6 TYPES OF WEAR IN THE COATING

The study of the processes of wear of coating is part of the discipline of Tribology. The complex nature of coating wear has resulted in isolated studies towards specific wear mechanisms or processes. Some wear mechanisms of coating include

1. Adhesive wear
2. Fatigue Wear
3. Fretting Wear
4. Diffusive Wear
5. Impact Wear
6. Erosive wear
7. Abrasive wear
8. Cavitation Wear

A number of different wear phenomena of coating are also commonly encountered and represented in literature. Impact wear, cavitations' wear, diffusive wear and corrosive wear are all such examples. These wear mechanisms; however, do not necessarily act independently in many applications. Wear mechanisms of the coatings are not mutually exclusive. "Industrial Wear" is the term used to describe the incidence of multiple wear mechanisms occurring in unison. Wear mechanisms and/or sub-mechanisms frequently overlap and occur in a synergistic manner, producing a greater rate of wear than the sum of the individual wear mechanisms.

### **1.6.1 Adhesive Wear**

This type of wear can be observed in the material from one surface to another during relative motion by a process of solid-phase welding or as a result of localized bonding between contacting surfaces. Removed particle from one surface are either permanently or temporarily attached to another surface. This wear causes high wear and friction coefficient to overcome these problems soft metal coating is introduced for this purpose, and Au, Ag, Pb and In are representative ones. One cannot observe the adhesion it two casually placed objects because of some contaminants like layer of oxygen and oil films. By increasing the hardness and surface roughness of contacting surface adhesion can be controlled. Adhesive wear of the coating can be described as plastic deformation of very small fragments within the surface layer when two surfaces slides against each other. The asperities (i.e., microscopic high points) found on the mating surfaces will penetrate the opposing surface and develop a plastic zone around the penetrating asperity. By increasing the hardness and surface roughness of contacting surface adhesion can be controlled.

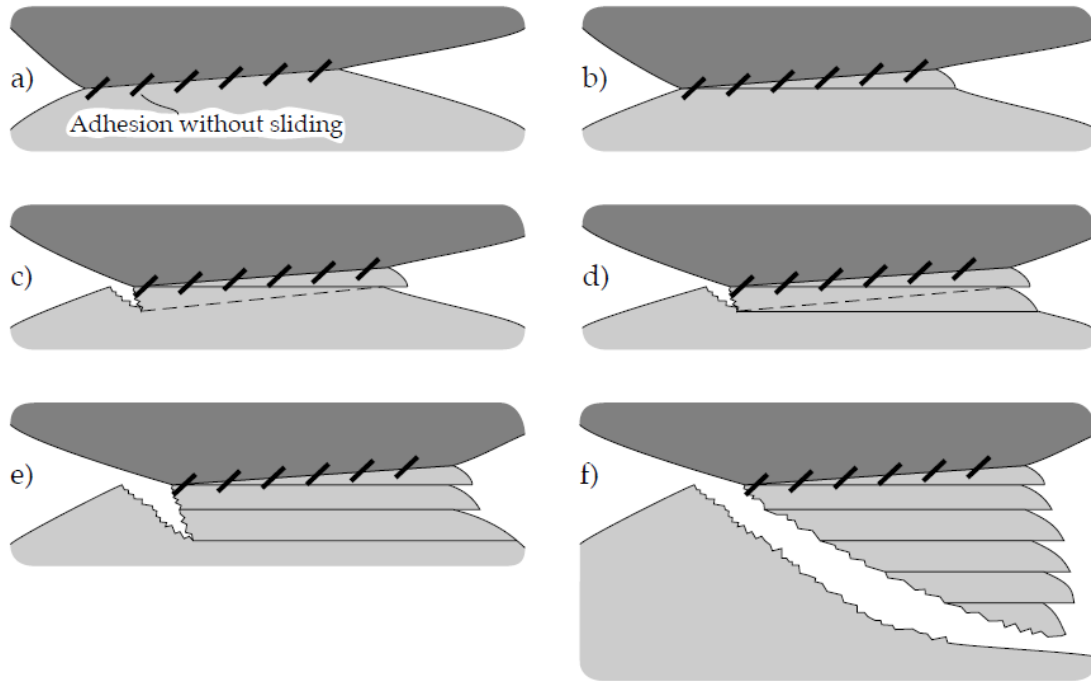


Figure 1.8: Schematic diagram of the formation of an adhesive transfer particle

### 1.6.1.1 Metal Transfer Mechanism

It is observed that before the transfer of a wear particle from one surface to another there will be a transfer film formation which characterizes and distinguishes the adhesive wear from other wear mechanisms. Earlier studies of adhesive wear were observed that brass rubbed against steel leaves a transferred film of brass on steel surface which are at wear track. The transferred brass was found to be highly work-hardened and probably capable of wearing the brass sample itself. This observation of inter-metallic transfer was confirmed later by tests on a variety of combinations of metals in sliding. Formation of wear metal and its removal is explained in schematic diagram in figure 1.9; shows that phenomena of negative wear rate in the form of transfer particle can lift the pin away from the opposing surface.

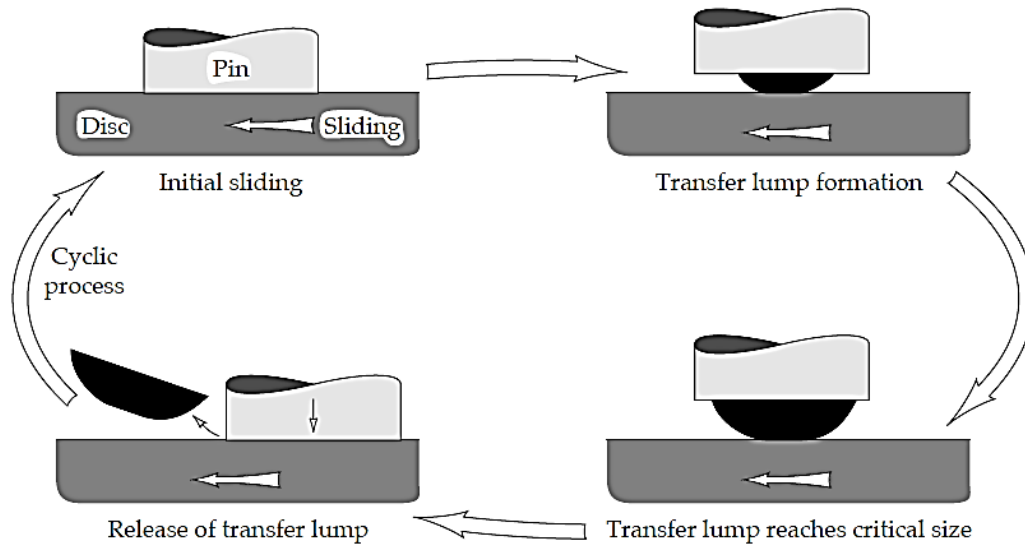


Figure 1.9: Formation and removal of a transfer particle

## 1.6.2 Fatigue Wear

Surface fatigue wear of the coating is a process by which the surface of coating is weakened by cyclic loading, which is one type of general material fatigue. Fatigue wear in coating is produced when the wear particles are detached by cyclic crack growth of micro cracks on the surface of the coating. These micro cracks are either superficial cracks or subsurface cracks. It is extremely important to improve the resistance of the material against fracture in aerospace applications and bearing failure caused by contact fatigue. In many well lubricated contacts adhesion between the two surfaces is negligible, yet there is still a significant rate of wear. This wear is caused by deformations sustained by the asperities and surface layers when the asperities of opposing surfaces make contact. Contacts between asperities accompanied by very high local stresses are repeated a large number of times in the course of sliding or rolling, & wear particles are generated by fatigue propagated cracks, hence 'fatigue wear'. Wear under these conditions is determined by the mechanics of crack initiation, crack growth and fracture.

To solve the fatigue damage problems of high-speed steels (HSS) the powder metallurgy (PM) routes are used. As a result of the finer and more uniform microstructure that PM-HSSs exhibit, as compared to their conventionally produced counterparts, they also present enhanced cross-sectional hardness uniformity (wear resistance), fracture toughness and fatigue strength [1].

### **1.6.3 Fretting Wear**

Fretting wear of the coating is the repeated cyclical rubbing between coating and another surface, which is known as fretting, over a period of time which will remove material from one or both surfaces in contact. It occurs typically in bearings, although most bearings have their surfaces hardened to resist the problem. Another problem occurs when cracks in either surface are created, known as fretting fatigue. Fretting occurs wherever short amplitude reciprocating sliding between contacting surfaces is sustained for a large number of cycles. It results in two forms of damage: surface wear and deterioration of fatigue life. The extent of wear and surface damage is much greater than suggested by the magnitude of sliding distance. Reciprocating movements as short as 0.1  $\mu\text{m}$  in amplitude can cause failure of the component when the sliding is maintained for one million cycles or more. Contacts which seem to be devoid of relative movement such as interference fits do in fact allow sliding on the scale of 1  $\mu\text{m}$  when alternating and oscillating loads are carried. It is very difficult to eliminate such movements and the resultant fretting. Fretting wear and fretting fatigue are present in almost all machinery and are the cause of total failure of some otherwise robust components. The fundamental characteristic of fretting is the very small amplitude of sliding which dictates the unique features of this wear mechanism. Under certain conditions of normal and tangential load applied to the contact a microscopic movement within the contact takes place even without gross sliding. The centre of the contact may remain stationary while the edges reciprocate with amplitude of the order of 1 $\mu\text{m}$  to cause fretting damage, fretting wear can be further accelerated by corrosion, temperature and other effects.

#### **1.6.3.1 Effect of Temperature on Fretting**

Contact point temperature plays a vital role between every moving surface whereas in fretting it can be observed in two ways, oxidation and corrosion rates which usually increases with temperature and second one is mechanical properties of metal which affected by the temperature. Fretting wear rate generally decreases with increase in temperature if an oxide film forms on the surface. The formation of protective films has been observed in high temperature fretting of, for example, carbon steel, stainless steel, titanium alloys and nickel alloy.

#### **1.6.4 Diffusive Wear**

When there is true contact between the atoms of opposing surfaces and a high interface temperature, significant diffusion of chemical elements from one body to another can occur. The most widespread example of such a contact is the rake face of a cutting tool close to the cutting edge in high speed machining. In this situation, there is almost the perfect contact between the tool and the metal chip due to the extreme contact stresses and very high temperatures, reaching 700°C or more. The metal chip represents a continually refreshed supply of relatively pure metal whilst the tool is a high concentration mixture of some radically different elements, e.g. tungsten and carbon. Therefore, there is a tendency for some of the elements in the tool to diffuse into the chip where solubility conditions are more favorable. When the surface material of the tool loses a vital alloying element it becomes soft and is very soon worn away by the chip.

#### **1.6.5 Impact Wear**

Impact wear is caused by repetitive collision between opposing surfaces. A classic example of this form of wear is found on the heads of hammers. This form of wear involves flat surfaces or nearly flat surfaces with a large radius of curvature compared to the size of the wear scar. This feature distinguishes impact wear from erosive wear where a sharp particle indents a flat surface. In impact wear the surface is subjected to repetitive impact by a series of pulses of high contact stress combined with some energy dissipation in each impact as shown schematically in Figure 1.10. The mechanism of impact wear involves elastic and plastic deformation when impact energy is high and/or fatigue accompanied by wear debris release due to crack formation. If oxygen is present and the wearing material can be oxidized then a corrosive or oxidative wear mechanism can also take place. Iron and steel components are susceptible to impact wear by tribo-oxidation especially at elevated temperatures at which rapid oxidation occurs. In general, impact wear is dependent on the formation of deformed layers, particularly when wear by fatigue or crack formation is predominant.



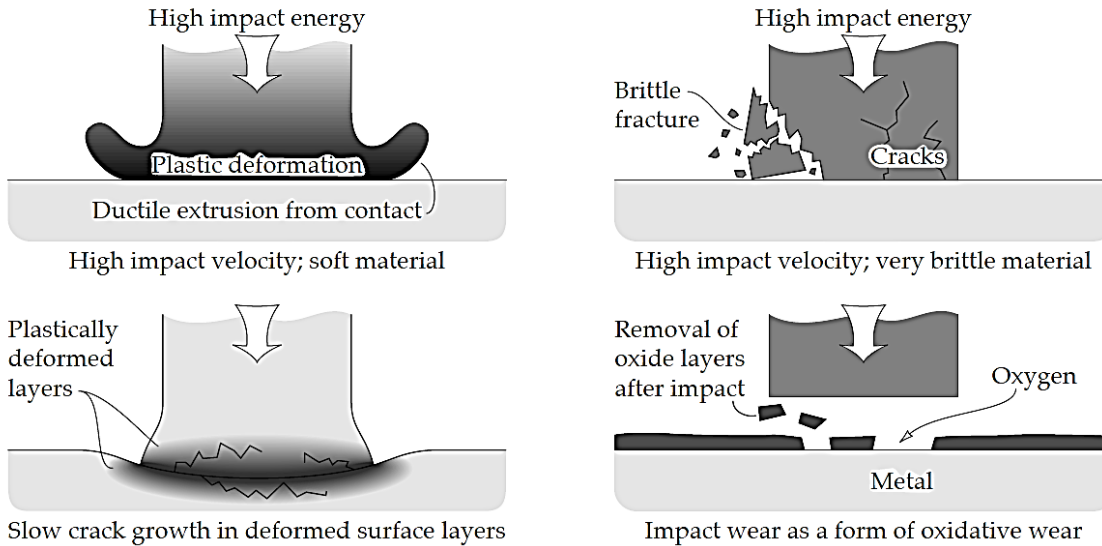


Figure 1.10: Schematic illustrations of the mechanisms of impact wear

### 1.6.6 Cavitation Wear

Cavitation wear is known to damage equipment such as propellers or turbine blades operating in wet steam, and valve seats. Wear progresses by the formation of a series of holes or pits in the surface exposed to cavitation. The entire machine component can be destroyed by this process. Operation of equipment, e.g. propellers, is often limited by severe vibration caused by cavitation damage. Cavitation wear can be accelerated by the simultaneous occurrence of erosive wear, in other words synergistic interaction between these two wear mechanisms is possible.

### 1.6.7 Erosive Wear

Erosive wear is caused by the impact of particles of solid or liquid against the surface of an object. Erosive wear occurs in a wide variety of machinery and typical examples are the damage to gas turbine blades when an aircraft flies through dust clouds, and the wear of pump impellers in mineral slurry processing systems. In common with other forms of wear, mechanical strength does not guarantee wear resistance and a detailed study of material characteristics is required for wear minimization. The properties of the eroding particle are also significant and are increasingly being recognized as a relevant parameter in the control of this type of wear. Erosive wear of the thermal spray coating is caused by the impact of particles of solid or liquid against the surface of coating [1].

### **1.6.7.1 Mechanism of Erosive Wear**

Erosive wear mechanism controlled by various factors like angle of impingement, material, impact velocity particle size and material. The term ‘erosive wear’ refers to an unspecified number of wear mechanisms which occur when relatively small particles impact against mechanical components. A low angle of impingement favors wear processes similar to abrasion because the particles tend to track across the worn surface after impact. A high angle of impingement causes wear mechanisms which are typical of erosion. The speed of the erosive particle has a very strong effect on the wear process. If the speed is very low then stresses at impact are insufficient for plastic deformation to occur and wear proceeds by surface fatigue. When the speed is increased to, for example, 20 m/s, it is possible for the eroded material to deform plastically on particle impact. In this regime, which is quite common for many engineering components, wear may occur by repetitive plastic deformation. If the eroding particles are blunt or spherical then thin plates of worn material. The size of the particle is also of considerable relevance and most of the erosive wear problems involve particles between 5 -500  $\mu\text{m}$  in size, although there is no fundamental reason why eroding particles should be limited to this size range.

### **1.6.8 Abrasive wear**

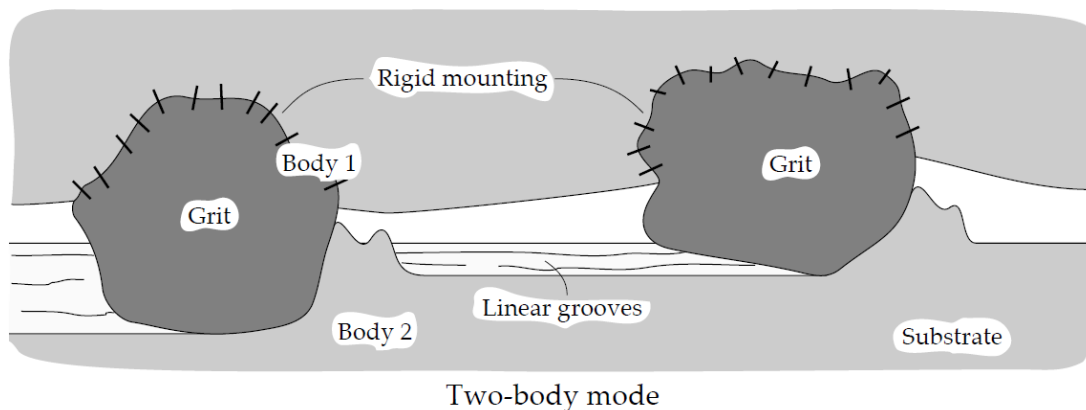
The abrasive wear of a material is defined as the progressive loss of material due to abrasive action of hard particles present between the counter surfaces. The abrasive wear depends on various factors like abrasive size, rake angle of abrasives, applied load and shape, size, volume fraction of the dispersed phases. In addition to these factors the abrasive wear rate of a material also depends on the surface hardness and materials properties like fracture toughness. A major difficulty in the prevention and control of abrasive wear is that the term ‘abrasive wear’ does not precisely describe the wear mechanisms involved [1]. There are, in fact, almost always several different mechanisms of wear acting in concert, all of which have different characteristics. The mechanisms of abrasive wear are described next, followed by a mode of wear.

### 1.6.8.1 Mechanisms of Abrasive Wear

It was originally thought that abrasive wear by grits or hard asperities closely resembled cutting by a series of machine tools or a file. However, microscopic examination has revealed that the cutting process is only approximated by the sharpest of grits and many other more indirect mechanisms are involved. The particles or grits may remove material by micro cutting, micro fracture, pull-out of individual grains or accelerated fatigue by repeated deformations. Literature denotes two basic modes of abrasive wear:

- Two-body and
- Three-body abrasive wear

Two-body abrasive wear is exemplified by the action of sand paper on a surface. Hard asperities or rigidly held grits pass over the surface like a cutting tool. In three-body abrasive wear the grits are free to roll as well as slide over the surface, since they are not held rigidly. Two-body abrasive wear corresponds closely to the ‘cutting tool’ model of material removal whereas three-body abrasive wear involves slower mechanisms of material removal, though very little is known about the mechanisms involved. It appears that the worn material is not removed by a series of scratches as is the case with two-body abrasive wear. The two and three-body modes of abrasive wear are illustrated schematically in Figure 1.11.



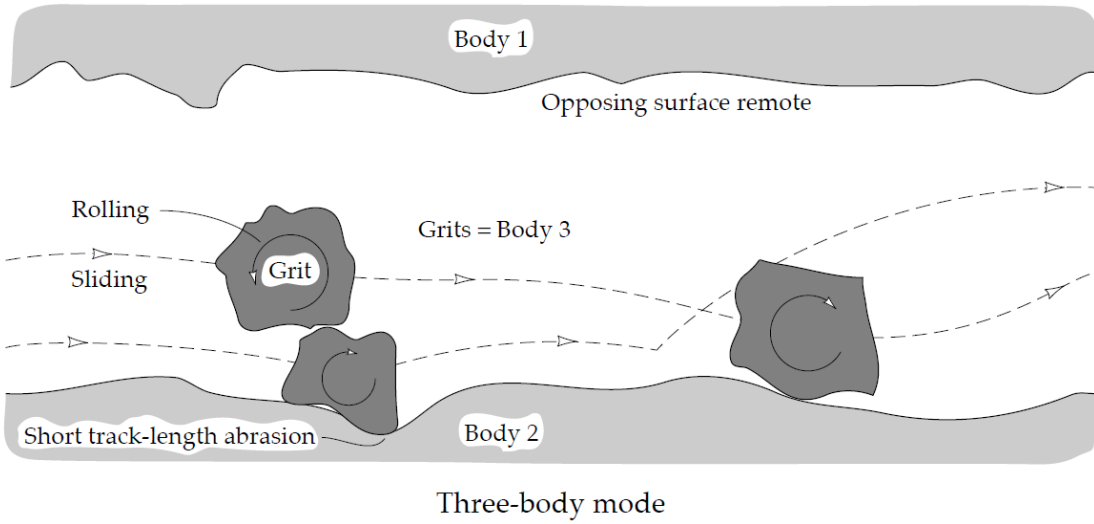


Figure 1.11: Two and three-body modes of abrasive wear

### LITERATURE REVIEW

**L.J. Yang (2005)** A test methodology is proposed in this paper to enable the wear coefficient to be determined more accurately, consistently, and efficiently. In this proposal, the wear test will be divided into three stages:

- (i) To conduct the transient wear test;
- (ii) To predict the steady-state wear coefficient with the required sliding distance by using the second wear coefficient equation proposed by Yang;
- (iii) To conduct the steady-state confirmation runs to obtain the measured steady-state wear coefficient value.

Based on the wear data obtained previously from aluminium based matrix composite materials, the average deviation between the predicted and measured standard steady-state wear coefficient values is found to be about 20%. The proposed methodology is found capable of saving about 40% of testing time if only the confirmation run at the predicted sliding distance is chosen.

**W. Grzesik et al. (2002)** The principle aim of this paper is to investigate three wear-protective coatings with multilayer structures, which are frequently used in the cutting tool industry and to assess their frictional behaviour under the test conditions equivalent to those for the cutting of medium carbon steel. A modified pin-on-disc tester was used to conduct experiments in which both the friction coefficient and the linear wear of the tribo-pair were recorded vs. sliding distance. The volumetric wear rate was proposed as a parameter for quantitative comparison of the wear resistance of the tribo-pairs tested. It was found that the principle stage of the specimen wear takes place during the first 200–240 s of sliding independently of the applied speed; obviously, after this stage the intensity of wear decreases drastically. The maximum values of specific wear rate observed at the lowest sliding speeds applied decrease significantly with the elevation of the sliding speed for all tribo-pairs, especially for coated specimens.

**C. Navas et al. (2005)** Laser surface treatments can be used as a powerful tool to repair moulds which have experienced severe damage during their service lifetime. The present paper studies the application of cladding techniques to repair moulds such as those used in the plastics industry. By means of a continuous wave diode laser operating at 600 W output power, a tool steel—annealed AISI A2—has been coated with two alloys with different protective properties: a high-speed steel with a high molybdenum content (AISI M2) and excellent mechanical properties; and a martensitic stainless steel (AISI 431) which combines good wear and corrosion resistance. After the treatment, the clad surfaces were characterized by means of optic and scanning electron microscopy. The layers showed a uniform composition across the track, similar to the initial powder composition, without damage or cracks. The mechanical properties were evaluated by hardness measurements and wear tests (ball-on-disk) at room temperature and without lubrication, in accordance with the ASTM G99-95a standard. The tribological couple was comprised by an alumina ball sliding against the clad layers. The wear rate varied with the different ball and disk combinations, and a considerable improvement in wear resistance was observed with the AISI M2 laser coatings compared with the substrate.

**L. J. Yang (2006)** A new equation has been formulated and found successful for modelling the wear rate of test specimens. It is capable of predicting the standard steady-state wear rate and the net steady-state wear rate with a FA value, an exponential function, of 0.99 and 0.999, respectively; and with deviations of about 19% and 36%, respectively. A methodology has also been proposed in this paper to enable the steady-state wear rate to be determined more accurately, consistently, and efficiently. The wear test will be divided into three stages:

- (i) To conduct the transient wear test;
- (ii) To predict the steady-state wear rate with the required sliding distance based on the transient wear data by using the new equation;
- (iii) To conduct confirmation runs to obtain the measured steady-state wear rate. The proposed methodology is supported by wear data obtained previously on aluminium based matrix composite materials. It is capable of giving more accurate steady state wear rates, as well as saving a lot of testing time and labor, by reducing the number of trial runs required to achieve the steady-state wear condition. It will also give more consistent results since a common Fa value will be used.

**A.W. Ruff (1997)** The large number of wear models found in the literature, no model can predict metal wear a priori based only on materials property data and contact information. The complexity of wear and the large number of parameters affecting the outcome are the primary reasons for this situation. This paper summarizes the current understanding of wear modelling for metals. Several recent approaches such as wear mapping and wear transition diagrams have suggested some future possible directions for improvement. Some success has been achieved in describing severe wear of steels under unlubricated conditions using thermo-mechanical approaches. However, modelling of mild wear remains problematic, especially under lubricated conditions. In mild wear, asperity contact events dominate the wear processes. A single asperity collision simulation apparatus has been used to study asperity-asperity contact phenomena. Shear strain and strain accumulation were found to be the dominant underlying causes for wear. It is proposed that future research in wear prediction for metals incorporate the following aspects: wear mapping, temperature, shear strain response, boundary lubricating film strength, and surface roughness.

**L.J. Yang (2003)** A new formulation of the wear coefficient was developed and tested experimentally. Two different types of pin-on-disc wear tests were conducted using three commercial, A6061 aluminium-based metal–matrix composites (MMCs). One type of test resulted in a spiral track and the other a circular track. Hardened tool steel discs were used as the sliding counter face for MMC pins having 10, 15 and 20% alumina reinforcements. A new wear equation was derived and shown to be a better predictor of steady-state wear coefficients. It is based on an exponential transient wear volume equation and Archard's equation.

**D.A. Stewart (1999)** WC–Co cermets have been used traditionally as wear-resistant materials. Recent work has shown that nanostructured cermets offer improved properties over their conventional counterparts. This work examines the performance of such conventional and nanostructured materials in the form of coatings deposited by high velocity oxy-fuel (HVOF) thermal spraying. WC–Co coatings were deposited under identical conditions using both conventional sintered and crushed and nanocomposite powder feed stocks. Both powders consisted of tungsten carbide (WC) grains in a cobalt binder. Characterization of the coatings by

a range of techniques showed that both coatings not only contained WC but also reaction products such as tungsten hemi carbide (W<sub>2</sub>C) and W and an amorphous Co-rich binder phase containing W and C. Due to differences in the morphology of the powder feedstock and the WC grain size, the nanocomposite coating contained a smaller fraction of unreacted WC than the conventional coating. Three body abrasive wear tests were performed using a modified dry sand rubber wheel apparatus with alumina and silica abrasives. A range of abrasive particle sizes and loads were used to assess the wear resistance of both coatings. It was found that the nanocomposite had a poorer wear resistance than the conventional coating under all the conditions examined. Wear was dominated by the loss of ductility in the Co-rich binder phase due to its amorphisation. The differences in the wear behaviour of the coatings could, thus, be explained in terms of differences in powder characteristics, the extent of reaction and decarburisation during spraying and the subsequent development of the microstructure in the coating during splat solidification at high cooling rates.

**L.J. Yang (2003)** Experimental pin-on-disc wear tests were carried out previously on three types of commercial A6061 aluminium-based matrix composites (MMCs) reinforced with 10, 15 and 20% alumina particles, respectively, against steel disc, with both the moving pin technique developed at Nanyang Technological University and the conventional pin-on-disc technique. An integrated wear model was established, with the transient wear volume described by an exponential equation while the steady-state wear by a revised Archard equation. A wear coefficient equation was formulated by using the transient wear data to model the standard wear coefficients of both the transient wear and the steady-state wear successfully. In this study, a new equation was developed from the previous model to predict the net steady-state wear coefficient. With a FA value of 0.999 or 0.9999, the average deviation from the measured values was about 26%. FA was an exponential function used in the transient wear equation. On the other hand, Peterson's equation was also found suitable for modelling the steady-state wear of the three types of aluminium based matrix composites. However it lacked some of the features the newly proposed equation could provide.



**Alfred Zmitrowicz (2006)** Wear is a process of gradual removal of a material from surfaces of solids subject to contact and sliding. Damages of contact surfaces are results of wear. They can have various patterns (abrasion, fatigue, ploughing, corrugation, erosion and cavitation). The results of abrasive wear are identified as irreversible changes in body contours and as evolutions of gaps between contacting solids. The wear depth profile of a surface is a useful measure of the removed material. The definition of the gap between contacting bodies takes into account deformations of bodies and evolutions of wear profiles. The wear depth can be estimated with the aid of wear laws. Derived in this study, constitutive equations of anisotropic wear are extensions of the Archard law of wear. The equations describe abrasion of materials with microstructures.

**M.Z. Huq (2001)** The wear of materials in sliding contacts is considered as resulting from an energy dissipation due to friction between the contacting first bodies. Up to now, no standard procedure in tribology is available to relate that dissipated energy with wear losses for different sliding wear tests and conditions. In this paper, a procedure is proposed to correlate the volumetric wear loss of one first body with the dissipated energy for unidirectional and bidirectional ball-on-flat tests. The model can be useful to predict the service lifetime of components from a limited number of laboratory tests. The validity and limitation of the wear loss versus dissipated energy model is illustrated for hard coatings like TiN and (Ti, Al)N, and multilayered (Ti, Al)N/TiN coatings. The effect of the applied normal load and the relative humidity (RH) of the ambient air on the wear rate for these different coatings is shown as well. A mild oxidational wear model is used to describe the material loss on these coatings in sliding contacts.

### MODELLING OF WEAR

Higher wear coefficient qualities can be gotten when the wear tests are done inside of the transient wear administration, or with an excessive sliding separation in the relentless state wear administration. It is likewise hard to judge whether the enduring state wear administration has been reached in directing the wear test. A test strategy is along these lines proposed in this paper to empower the wear coefficient to be resolved all the more precisely, reliably, and productively. In this proposition, the wear test will be partitioned into three stages:

- i. To direct the transient wear test
- ii. To foresee the enduring state wear coefficient with the obliged sliding separation by utilizing the second wear coefficient mathematical statement proposed by Yang; and
- iii. To direct the enduring state affirmation rushes to get the deliberate relentless state wear coefficient esteem.

Taking into account the wear information got beforehand from aluminium based grid composite materials, the normal deviation between the anticipated and measured standard steady-state wear coefficient qualities is discovered to speak the truth 20%. Wear testing is a period expending procedure, as the test must be rehashed with diverse sliding separation until a steady state wear condition is accomplished. Besides, it might likewise be difficult to judge accurately whether a consistent state wear condition has really been accomplished. Figure 3.1(a) demonstrates that a wear volume versus separation bend can for the most part be isolated into two administrations, the transient wear administration and the consistent state wear administration. The standard wear coefficient esteem obtained from a volume misfortune versus separation bend is a component of the sliding separation. Because of the higher starting running-in wear rates, it has a higher esteem at first and will achieve a steady state value when the wear rate gets to be consistent, as shown in Figure 3.1(b). This is on the grounds that the standard technique to calculate the wear coefficient is to make utilization of the aggregate volume loss and the aggregate sliding separation secured. Then again, it is

obvious from Figure 3.1(b) that the standard wear coefficient quality acquired would be higher if the sliding separation secured remains within the transient wear administration. Then again, extreme separation would likewise harm the wear track to give a higher wear coefficient. Henceforth, it is not astounding that wear coefficient qualities got from diverse specialists have been found to change essentially up to a deviation of 1000%. As there is an absence of a standard test technique accessible for the determination of the wear coefficient of a wearing pair, it is high time to investigate it. Standard testing practice has a tendency to perform the wear test just in the alleged "consistent state" region without knowing precisely where the relentless state regime is found. Thus, under-tried condition or over-tried conditions are regularly utilized. These won't offer ascent to accurate results as specified prior. Moreover, time and resources are also wasted all the while.

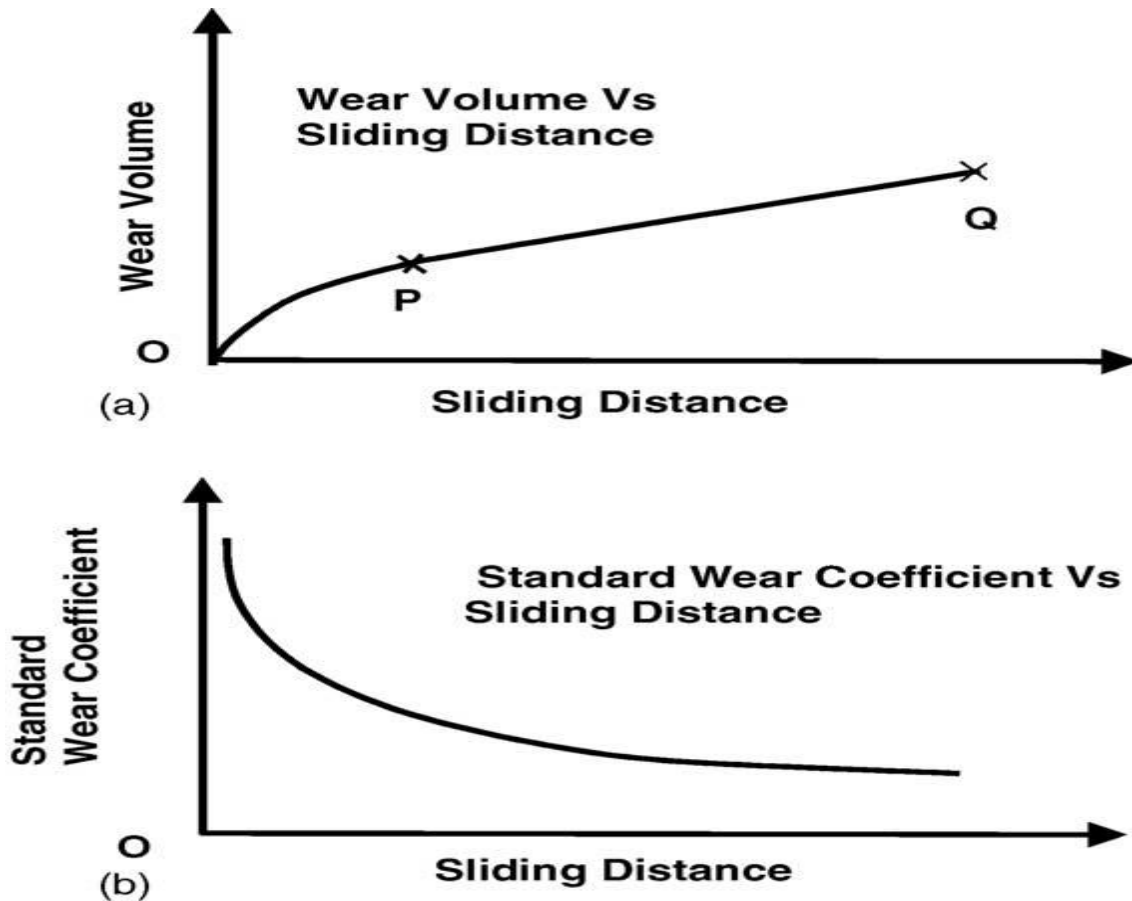


Figure 3.1: (a) Wear volume versus sliding distance; (b) standard wear coefficient versus sliding distance.

### 3.1 The Integrated Wear Model

The coordinated cement wear model was proposed by the author in the past studies to empower the net relentless state wear coefficient to be resolved all the more exactly, based on the consistent state wear volume and sliding separation only. Figure 3.2 shows the incorporated transient and unfaltering state adhesive wear model, which is likewise alluded as the incorporated adhesive wear model. The wear volume curve is comprised of two sections, the transient wear administration and the unfaltering state wear administration [5].

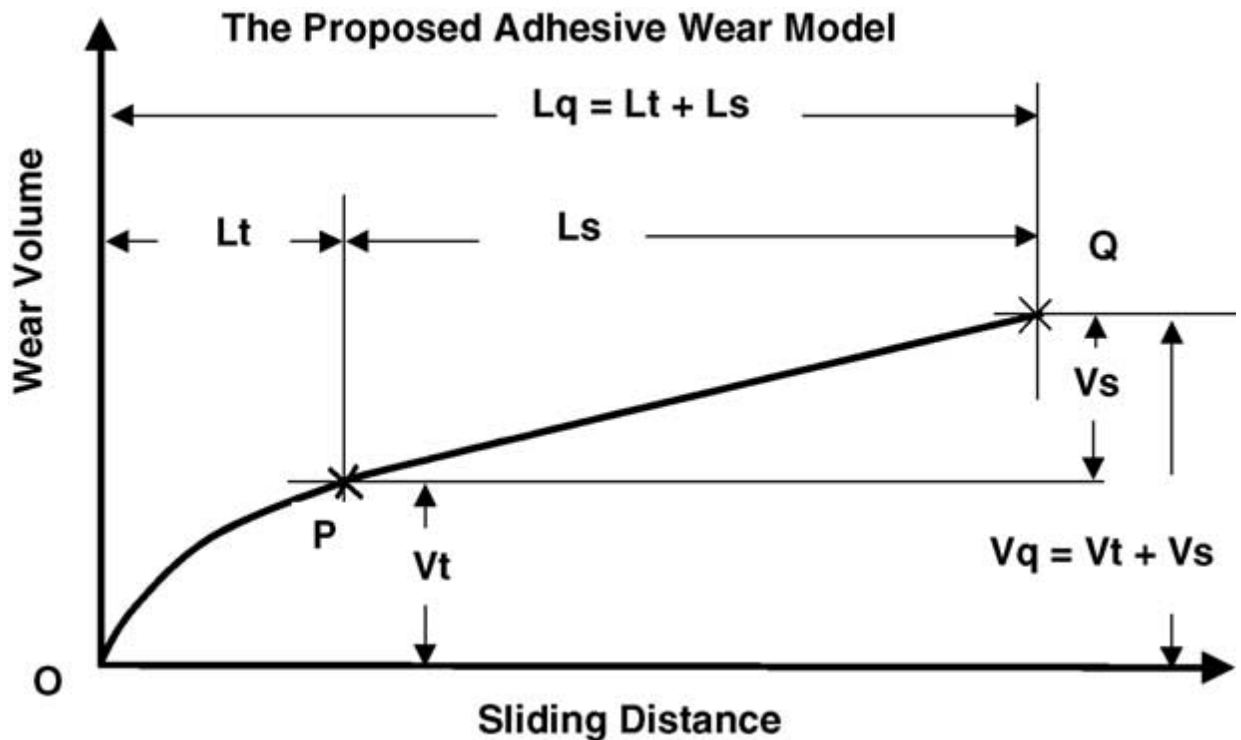


Figure 3.2: The Integrated wear model.

The volume misfortune is at first curvilinear and the rate of volume misfortune per unit sliding separation diminishes until at P where it joins easily with the straight line PQ. Henceforth, point P speaks to the end of transient wear and  $L_t$  is the transient wear separation. Point P likewise speaks to the start of the unfaltering state wear. At point Q, the example will have secured an aggregate sliding separation of  $L_q$  and the aggregate volume misfortune will be  $V_q$ .

### 3.2 The Transient Wear

In the glue wearing procedure, touching severities follow together first; and the plastic shearing of the intersections so framed will "cull" off the tips of the gentler asperities leaving them holding fast to the harder surface. Thusly, these tips can get to be confined offering ascent to wear particles or sections to bring about wear volume misfortune. The inference of the transient wear mathematical statement, it can be expected that the rate of volume uprooted per unit sliding separation is an element of the volume of metal accessible at the intersections.

$$(dV|dL) = -BV \quad (1)$$

Where V indicates the volume, L the sliding separation and B is a consistent who relies on upon the connected burden and the surface condition of the wear surface. The negative sign depicts a situation where the first volume at the intersections diminishes with sliding separation. It is accepted that A is the volume at the intersections at zero sliding separation and  $V_t$  is the transientwear volume (i.e. the volume evacuated) at a sliding distance L. By coordinating Eq. (1) and applying the limit conditions, one gets Eq. (2) where L ought to be equivalent to or less than  $L_t$ , which is the transient wear separation [3].

$$V_t = A[1 - e^{-BL}] \quad (2)$$

### 3.3 STEADY-STATE WEAR

#### 3.3.1 Standard Wear Coefficient ( $K_S$ )

For relentless state wear, Eq. (3) was proposed by Archard

$$V = K_S \frac{PL}{3H} \quad (3)$$

Where 'V' is the volumetric loss of the softer material subsequent to sliding for separation 'L' at load 'P' typical to the wear surface. H is the Brinell hardness of the milder wearing material while  $K_S$  is a dimensionless standard wear coefficient portraying the specific pin-circle interface. For known estimations of V, P, L and H, the standard wear coefficient ( $K_S$ ) can be figured from Eq. (4). For a specific material, it ought to be noticed that V could be assessed from the weight reduction W and the density  $\rho$ .

$$K_s = \frac{3HV}{PL} \quad (4)$$

### 3.3.2. Net Steady-State Wear Coefficient ( $K_N$ )

As Archard's comparison in its present structure would for the most part give higher "gross" relentless state wear coefficient esteem, there is a need to characterize the net consistent state wear coefficient. To display the net consistent state wear, Eq. (5) is utilized to speak to the consistent state wear volume,  $V_s$ .

$$V_s = K_N \frac{PL_s}{3H} \quad (5)$$

Where  $V_s$  and  $L_s$  are separately the consistent state wear volume and sliding separation as demonstrated in Fig. 2. Both  $V_s$  and  $L_s$  can be computed by utilizing Equations. (6) And (7), individually.  $K_N$  is the dimensionless net consistent state wear coefficient, which can be registered from Eq. (8) once  $V_s$  and  $L_s$  are known. It is a more exact wear parameter, which will encourage a superior examination of the wear properties of diverse pin materials.

$$L_s = L_q - L_t \quad (6)$$

$$V_s = V_q - V_t \quad (7)$$

$$K_N = \frac{3HV_s}{PL_s} \quad (8)$$

### 3.4 Transient Distance

To focus the transient separation, it is accepted that the sliding separation  $L = L_t$  is the end of the transient wear and start of relentless state wear. From Fig. 2, it is clear that at  $L = L_t$  the inclination of transient wear is equivalent to the angle of the consistent state wear. Consequently Eq. (9) can be determined by separating Equations. (2) And (8), and after that comparing them.

$$L_t = \frac{-\ln\left[\frac{V_s}{AB L_s}\right]}{B} \quad (9)$$

Eq. (9) shows that the transient separation  $L_t$  can be resolved if the constants A and B and additionally the  $L_s$  and  $V_s$  qualities are known. A and B qualities can be gotten from the separate transient volume misfortune versus separation information by utilizing a standard business programming. Be that as it may, both  $L_s$  and  $V_s$  values can't be resolved from Equations. (6) And (7) without an  $L_t$  esteem. To beat this trouble, various rough transient separation values ( $L_{ta}$ ) can be expected to work out some surmised  $L_{sa}$  and  $V_{sa}$  values. With these qualities, various transient separation ( $L_t$ ) qualities can be found from Eq. (9). The normal  $L_t$  Worth is then used to ascertain the  $L_s$  and  $V_s$  values, by utilizing Equations. (6) And (7), separately. Thusly, the net consistent state wear coefficient ( $K_N$ ) can be processed from Eq. (8). It ought to be noticed that the decision of  $L_{ta}$  is not discriminating and it won't influence the computed results essentially. This is on the grounds that the unfaltering state wear volume, as communicated by Eq. (3), for the most part has a straight relationship.

### 3.5 Second Wear Coefficient Equation

The main wear coefficient comparison proposed by Yang was in view of the numerical model for the transient wear volume. It was utilized for displaying the wear coefficient estimations of an Al-Al<sub>2</sub>O<sub>3</sub>/steel composite framework. Taking after the same strategy utilized already, Eq. (10) was produced with Eq. (2) as the transient comparison. This mathematical statement has numerous points of interest over the first because of the accompanying reasons. As a matter of first importance, the circulation of particles in a metal network composite is dependably non uniform, to give diverse volume portion values starting with one segment then onto the next. Next, distinctive molecule sizes are available in a specific segment. Besides, just two slopes are utilized as a part of the first mathematical statement to characterize the transient bend. This may not give a precisely characterized arch. On account of Eq. (10), just two parameters (A and B) should be resolved. It is additionally nonexclusive in nature with the capacity to display different combinations and materials. With the utilization of a set up programming, the estimations of A and B, that is the state of the transient bend, can be resolved all the more precisely as all the transient information points are completely used to acquire the 'best-fit' bend to give more accurate results. Henceforth, Eq. (10) will be utilized as a part of this study instead.

$$K_s = \frac{3HA[1-e^{-BL}]}{PL} \quad (10)$$

### 3.6 Effect of Exponential Factor $F_A$

Eq. (10) demonstrates that the wear coefficient esteem reachable will rely on upon the  $F_A/L$  esteem, where  $F_A$  is characterized in Eq. (11). The  $F_A$  worth will just increment gradually after the starting period. Moreover,  $F_A$  can just have a greatest estimation of solidarity. Henceforth, the estimation of  $F_A/L$  will decline further as the separation (L) is expanded, and will turn into zero when L is at limitlessness.

$$F_A = [1 - e^{-BL}] \quad (11)$$

Eq. (10) can be re-composed as:

$$K_P = \frac{3HA[1 - e^{-BL_P}]}{PL_P} \quad (12)$$

Where  $K_P$  is the anticipated unfaltering state wear coefficient,  $L_P$  is the anticipated sliding separation, and the  $F_A$  quality is demonstrated by the term  $[1 - e^{-BL}]$ . It can be demonstrated that Eq. (13), in which C is a steady that is equivalent to 4.605, 6.908 and 9.210 for a  $F_A$  estimation of 0.99, 0.999 and 0.9999, individually, is the general comparison that can be utilized to focus the predicted sliding separation  $L_P$ . By substituting Eq. (13) into Eq. (12), one gets Eq. (14), in which  $K_P$  is the anticipated wear coefficient value, D is a consistent which is equivalent to 0.215, 0.145 and 0.109 for an  $F_A$  estimation of 0.99, 0.999 and 0.9999, separately [5]. It ought to additionally be noted that this pretty nearly level with to  $1/C$ . Past work has likewise demonstrated that, the best  $F_A$  value for the determination of the anticipated standard unfaltering state wear coefficient quality is 0.99 while the best  $F_A$  esteem for the determination of the anticipated net standard relentless state wear coefficient worth is 0.999 or 0.9999.

$$L_P = \left[ \frac{C}{B} \right] \quad (13)$$

$$K_P = \frac{3HABD}{P} \quad (14)$$



**RESULT AND DISCUSSION**

**4.0 LOAD VS. VOLUME LOSS**

Different curves are drawn by using the experimental values.

**Table 4.1: For Cast iron**

Load( in 'N')	Volume Loss (in ' $mm^3$ ')	Volume Loss (in ' $mm^3$ ')	Volume Loss (in ' $mm^3$ ')
	Sliding Velocity( $V_s=1m/s$ )	Sliding Velocity( $V_s=2m/s$ )	Sliding Velocity( $V_s=3m/s$ )
50	4.5	6	6.9
60	5.1	6.8	7.6
70	6	7.5	8.2
80	6.6	8.3	9
90	7	9	9.5
100	8	9.5	10.2

These Values show an increasing trend for volume loss. Also as the sliding velocity is increased by increasing the rpm value for disc the volume loss increases for a particular load. The rpm values varied are 319 rpm, 764 rpm and 1433 rpm. The graphs are also plotted against load vs. volume loss for different sliding velocities i.e. for 1m/s, 2m/s, 3m/s. A similar trend had seen in case of chromium-nitride coating and similar graphs are plotted for chromium nitride coating i.e. for 1m/s, 2m/s, 3m/s.

Standard wear coefficient firstly introduced by Archard and then used by L.Y yang for different experiments by varying sliding distance and keeping load and sliding velocity same. A similar approach is used to find out the variation of second wear coefficient vs. load keeping sliding velocity constant for the first case. In the second case graph made for standard wear coefficient vs. Volume loss for different-2 velocities.

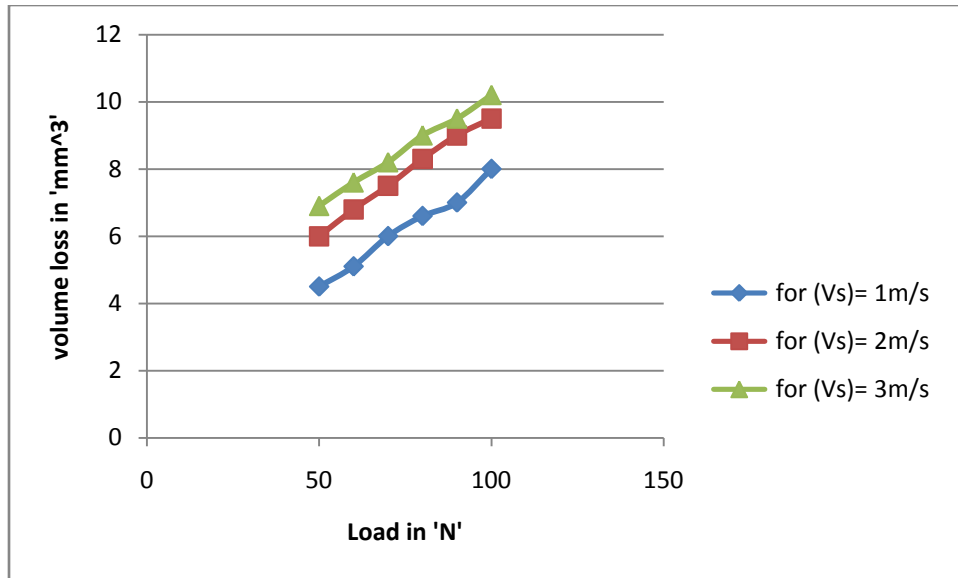


Figure 4.1: Volume loss vs. Load for different sliding velocities for Cast iron.

**Table 4.2: For chromium nitride coating**

Load( in 'N')	Volume Loss (in ' $mm^3$ ')	Volume Loss (in ' $mm^3$ ')	Volume Loss (in ' $mm^3$ ')
	Sliding Velocity( $V_s=1m/s$ )	Sliding Velocity( $V_s=2m/s$ )	Sliding Velocity( $V_s=3m/s$ )
50	4	5.3	6.2
60	4.7	6	6.8
70	5.2	6.8	7.5
80	6	7.3	7.9
90	6.9	8	8.2
100	7	8.4	8.7

As seen from the above table the values also show an increasing trend for Load vs. Volume loss for a particular sliding velocity. But the values are lower as compared to the Cast iron values.

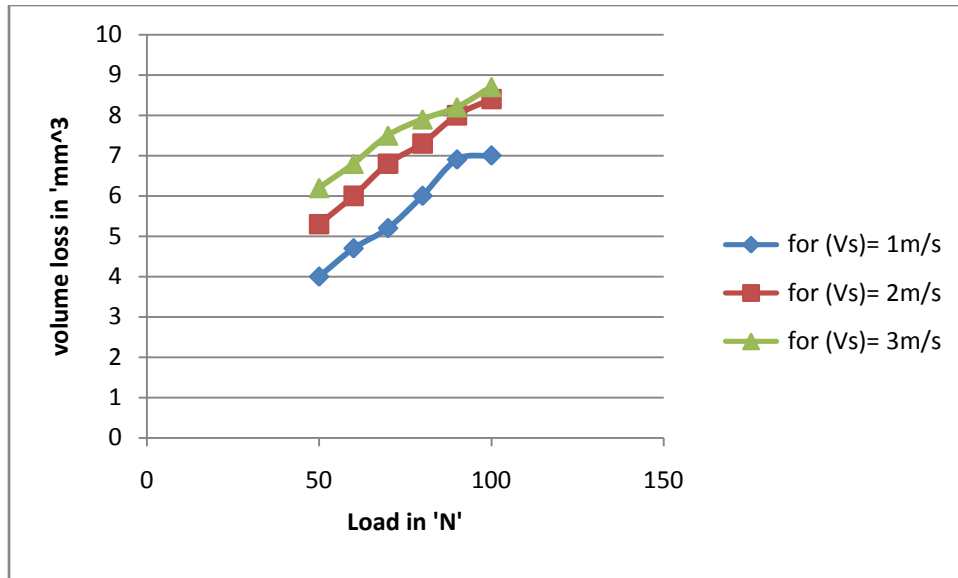


Figure 4.2: Volume loss vs. Load for different sliding velocities for chromium.

#### 4.1 STANDARD WEAR COEFFICIENT VS. VOLUME LOSS

Table 4.3: For Cast iron at sliding velocity of 1m/s

Volume Loss (in ' $mm^3$ ')	Standard Wear Coefficient $\times (10^{-5})$
4.5	7.56
5.1	7.14
6	7.2
6.6	6.93
7	6.53
8	6.72

Above Table shows a decreasing trend for second wear coefficient with volume loss at the sliding velocity of 1m/s.

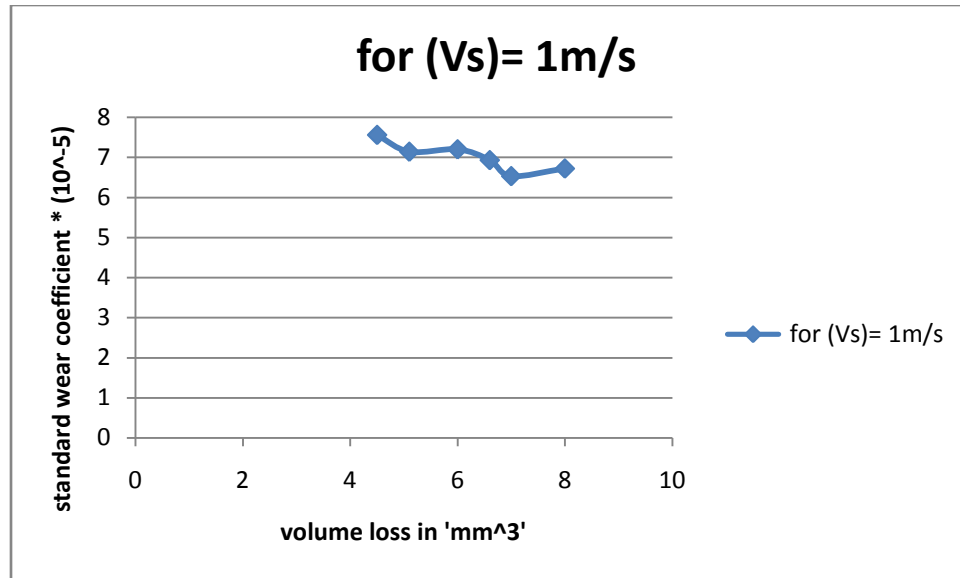


Figure 4.3: Standard wear coefficient vs. Volume Loss for Cast iron.

**Table 4.4: For chromium nitride coating at sliding velocity of 1m/s**

Volume Loss (in 'mm <sup>3</sup> ')	Standard Wear Coefficient *(10 <sup>-5</sup> )
4	6.72
4.7	6.58
5.2	6.24
6	6.3
6.9	6.44
7	5.88

The values of standard wear coefficient for chromium nitride coating are lower than Cast iron. These values also shows decreasing trend with volume loss. For the calculation of standard wear coefficient for chromium nitride coating the hardness of iron is considered as in the formula brinell hardness no. For softer material is considered and brinell hardness value for iron is less as compare to chromium nitride coating. Equation (4) is used to find out the standard wear coefficient.

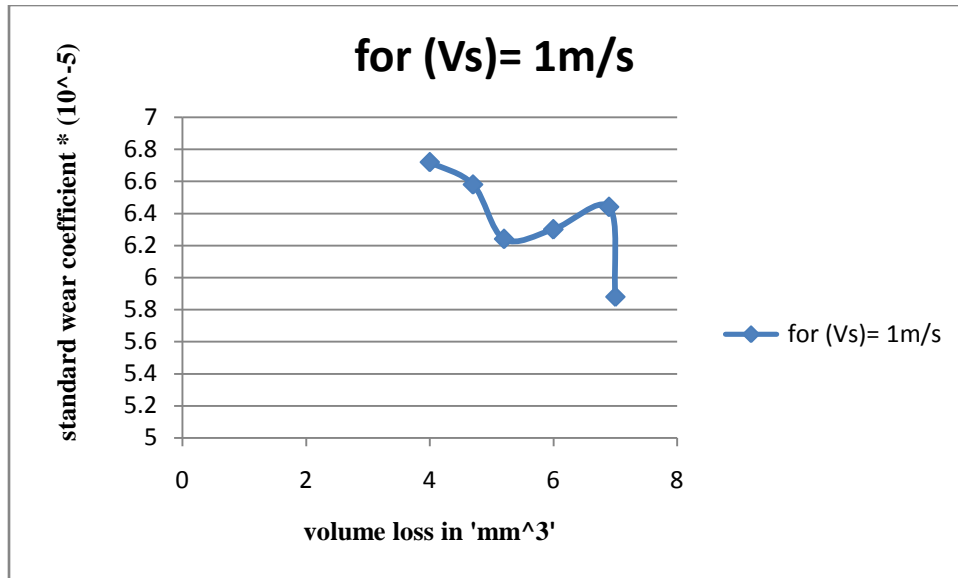


Figure 4.4: Standard wear coefficient vs. Volume Loss for chromium nitride.

**Table 4.5: For Cast iron at sliding velocity of 2m/s**

Volume Loss (in 'mm <sup>3</sup> ')	Standard Wear Coefficient *(10 <sup>-5</sup> )
6	10.08
6.8	9.52
7.5	9
8.3	8.715
9	8.4
9.5	7.98

Volume loss and standard wear coefficient values at sliding velocity 2m/s are higher as compare to at 1m/s. But with increasing volume loss the second wear coefficient values decreases.

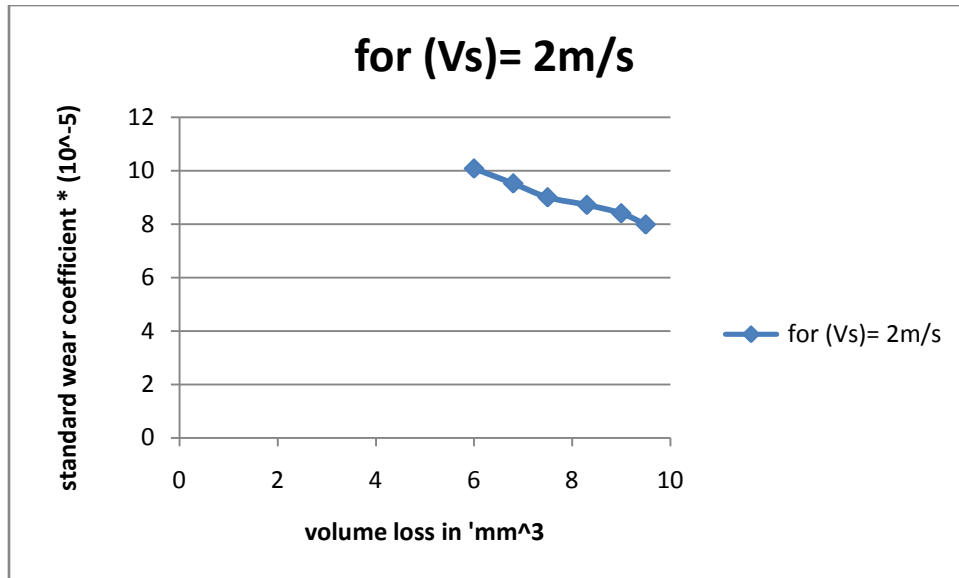


Figure 4.5: Standard wear coefficient vs. Volume Loss for Cast iron.

**Table 4.6: For chromium nitride coating at sliding velocity of 2m/s**

Volume Loss (in 'mm <sup>3</sup> ')	Standard Wear Coefficient *(10 <sup>-5</sup> )
5.3	8.904
6	8.4
6.8	8.16
7.3	7.665
8	7.47
8.4	7.056

The values of standard wear coefficient are lower as compare to Cast iron at same sliding velocity of 2m/s.

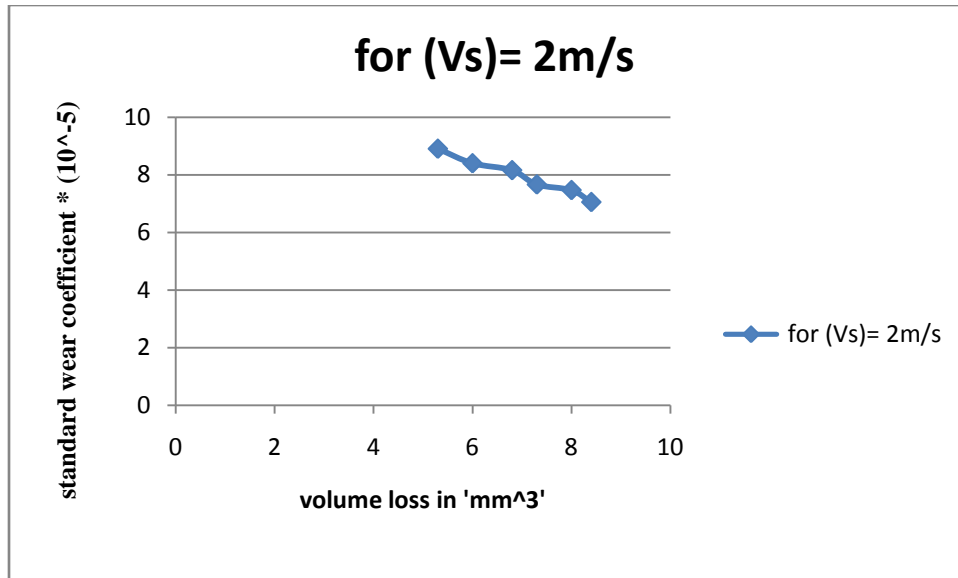


Figure 4.6: Standard wear coefficient vs. Volume Loss for chromium nitride.

**Table 4.7: For Cast iron at sliding velocity of 3m/s**

Volume Loss (in 'mm <sup>3</sup> ')	Standard Wear Coefficient *(10 <sup>-5</sup> )
6.9	11.6
7.6	10.64
8.2	9.84
9	9.45
9.5	8.87
10.2	8.57

As the volume loss increases with load applied the second wear coefficient value decreases with increase in load value. The volume loss increases with increase in load but the fraction of volume loss to load decreases as load increase is much higher as compare to volume increase thereby decreasing the standard wear coefficient.

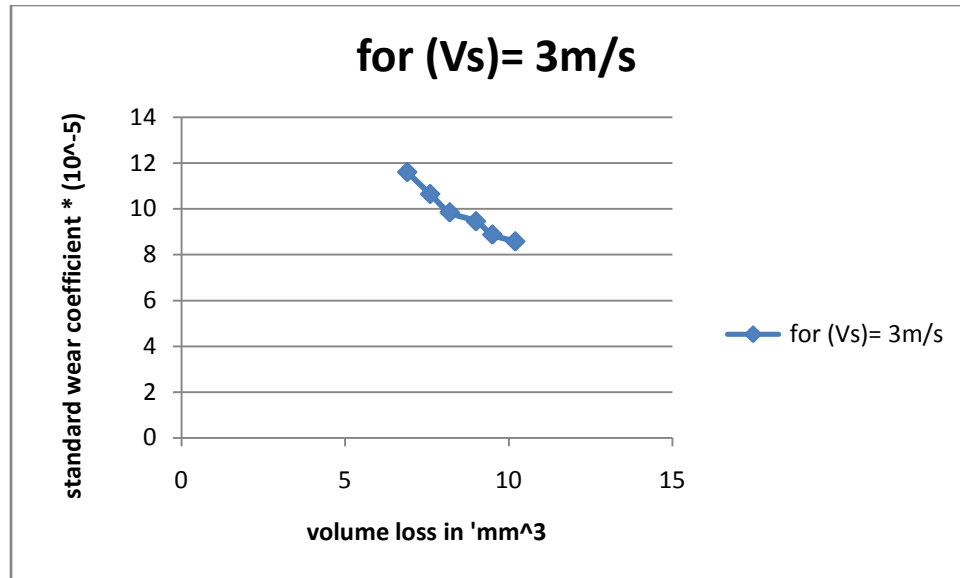


Figure 4.7: Standard wear coefficient vs. Volume Loss for Cast iron.

**Table 4.8: For chromium nitride coating at sliding velocity of 3m/s**

Volume Loss (in 'mm <sup>3</sup> ')	Standard Wear Coefficient *(10 <sup>-5</sup> )
6.2	10.416
6.8	9.52
7.5	9
7.9	8.295
8.2	7.65
8.7	7.308



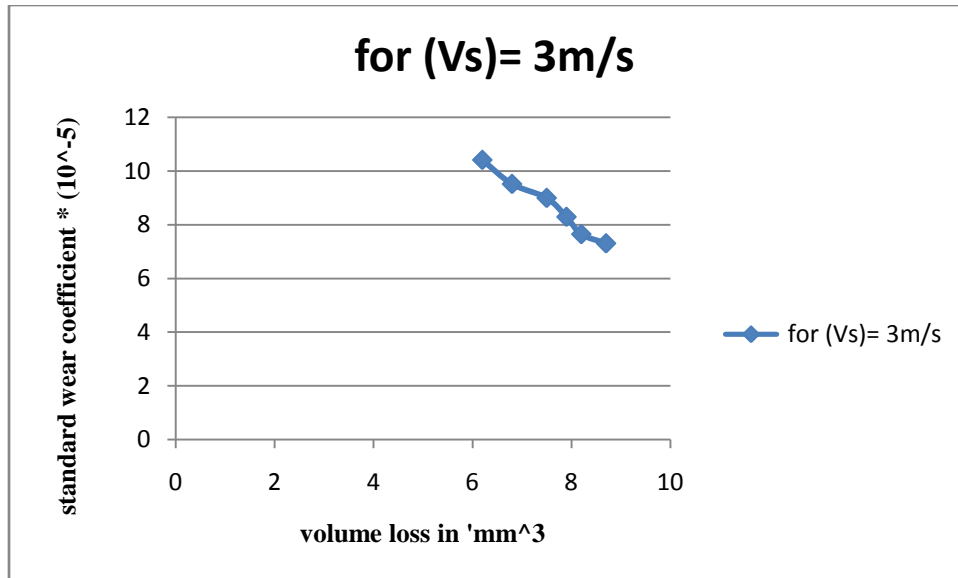


Figure 4.8: Standard wear coefficient vs. Volume Loss for chromium nitride.

From the above graphs of standard wear coefficient vs. Volume loss for sliding velocities 1m/s, 2m/s, 3m/s there is good agreement between the curves formed for Cast iron and chromium nitride coating. The graphs between volume loss vs. Load for Cast iron and chromium nitride coating also shows a good agreement.

## 4.2 LOAD VS. AVERAGE STANDARD COEFFICIENT

Table 4.9: For Cast iron

Load( in 'N')	Average standard coefficient( $K_s$ ) $\times (10^{-5})$
50	9.75
60	9.1
70	8.68
80	8.365
90	7.93
100	7.76

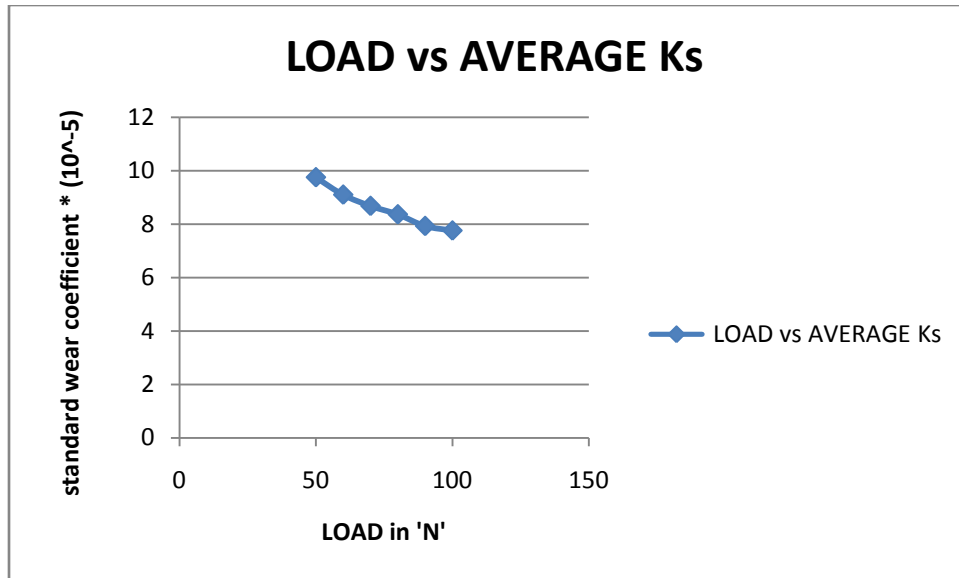


Figure 4.9: Load vs. Standard wear coefficient for Cast iron.

**Table 4.10: For chromium nitride coating**

Load( in 'N')	Average standard coefficient( $K_s$ ) *(10 <sup>-5</sup> )
50	8.904
60	8.4
70	8.16
80	7.665
90	7.47
100	7.056

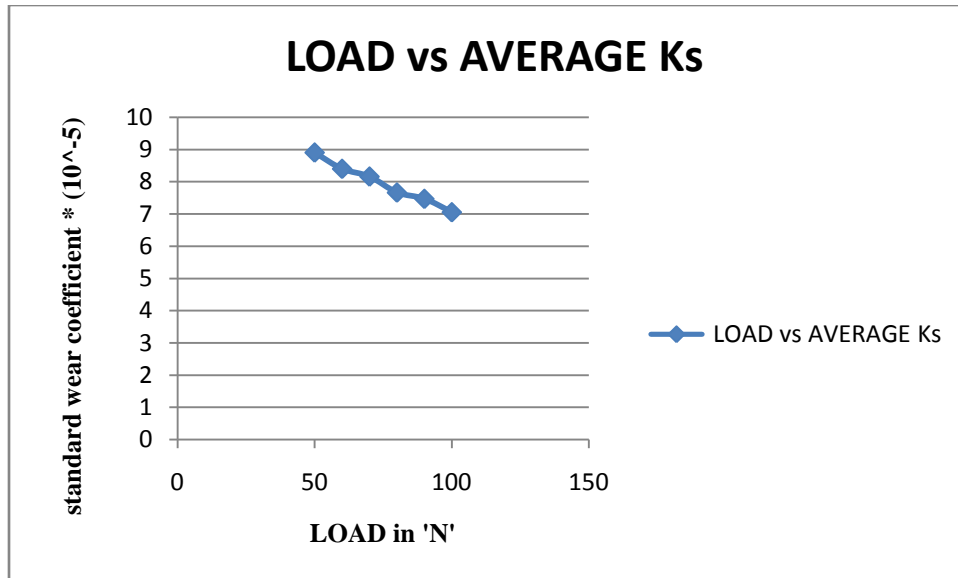


Figure 4.10: Load vs. Standard wear coefficient for chromium nitride coating.

The variation for Load and Standard wear coefficient for iron and chromium nitride coating shows a good agreement between them.

Standard Wear Coefficient (Probability Factor) not every contact results in a wear particle. It is assumed that a proportion **Ks** (independent of their size) does so. **K** may therefore be regarded as a probability factor typical of the combination of materials used, applying over a range of experimental conditions where the wear process remains of the same type. The derivation of Standard wear coefficient uses the “foregoing theory”. It is this mechanism which gives a wear/load relationship in accord with the experimental evidence. From the values obtained for average value of standard wear coefficient for cast iron and chromium nitride coating there is a reduction in wear of 8.67% by using chromium nitride coating for load 50N, 7.69% for load 60N, 6% for load 70N, 8.36% for load 80N, 5.80% for load 90N, 9.07% for load 100N.

An average reduction of 7.60% in wear takes place by using chromium nitride coating instead of cast iron which provides better option over cast iron.

### 4.3 CONCLUSION

1. The Standard Wear Coefficient also called “Probability Factor” by Archard decreases with increasing load. It means that the proportion of contact points which are undergoing plastic deformation and causing wear decreases.
2. In the case of dissimilar metals the deduced values of standard wear coefficient are about 0.1 percent or less, but the experimental evidence is that this reduction is largely due to the reduced size rather than the number of the particles.
3. The values of standard wear coefficient indicate the degree to which the transfer or wear is reduced below the maximum expected value and so provide a qualitative basis for the assessment of the experimental results.
4. J.F Archard assumed that if standard wear coefficient is constant the volume loss is independent of sliding speed but above results show that standard wear coefficient and volume loss varies with sliding speed.
5. With increasing load the volume loss increases but the amount of volume loss is less incremented as compare to the load which leads to the decreasing trend for standard wear coefficient.

## REFERENCES

---

---

1. Stachowiak, G. W, and A. W Batchelor; Engineering Tribology, Butterworth-Heinemann, Boston, 2014, ISBN 9780123970473.
2. W. Grzesik, Z. Zalisz, P. Nieslony Friction and wear testing of multilayer coatings on carbide substrates for dry machining applications, 2002.
3. L.J. Yang, Wear coefficient equation for aluminum-based matrix composites against steel disc, doi: 10.1016/S0043-1648(03)00191-1.
4. L.J. Yang, Prediction of net steady-state wear coefficient in an Al-Al<sub>2</sub>O<sub>3</sub>(P)/steel system with an integrated wear model, Tribology Letters, Vol. 17, No. 2, August 2004.
5. L.J. Yang, A test methodology for the determination of wear coefficient, doi:10.1016/j.wear.2005.01.026.
6. L. J. Yang, Determination of Steady-State Adhesive Wear Rate, doi: 10.1115/1.2345410.
7. M.Z. Huq, Expressing wear rate in sliding contacts based on dissipated energy Wear 252 (2002) 375–383.
8. Alfred Zmitrowicz, journal of theoretical and applied mechanics 44, 2, pp. 219-253, warsaw 2006.
9. C. Navas, Laser coatings to improve wear resistance of mould steel, doi:10.1016/j.surfcoat.2004.05.002.
10. M. C. Shen, Wear prediction for metals, Tribology International Vol. 30, No. 5, pp. 311-383, 1997.
11. Donald M. Mattox; Handbook of Physical Vapor Deposition (PVD) Processing (Second Edition), William Andrew Publishing, Boston, 2010, ISBN 9780815520375.
12. Bhushan, Bharat, and B. K Gupta. Handbook of Tribology: Materials, Coatings, and Surface Treatments. New York: McGraw-Hill, 1991. ISBN 97815752405035.
13. J.F. Archard, Single Contacts and Multiple Encounters, Journal of Applied Physics, Volume 90, Issues 1–2, 15 March 1997, Pages 156-163, ISSN 0257-8972, [http://dx.doi.org/10.1016/S0257-8972\(96\)03112-X](http://dx.doi.org/10.1016/S0257-8972(96)03112-X)

14. Archard, J. F. 'Contact and Rubbing of Flat Surfaces'. *Journal of Applied Physics*. Volume 24. Issue 8 (1953): 981-988. <http://dx.doi.org/10.1063/1.1721448>.
15. C Friedrich, G Berg, E Broszeit, F Rick, J Holland, PVD CrxN coatings for tribological application on piston rings, *Surface and Coatings Technology*, Volume 97, Issues 1–3, December 1997, Pages 661-668, ISSN 0257-8972.
16. Donald M. Mattox, 'Fundamentals of Ion Plating'. *Journal of Vacuum Science & Technology*. Volume 10. Issue 1, 1973, Page 47.
17. Donald M. Mattox; *Handbook of Physical Vapor Deposition (PVD) Processing (Second Edition)*, William Andrew Publishing, Boston, 2010, ISBN 9780815520375.
18. K.O. Legg, M. Graham, P. Chang, F. Rastagar, A. Gonzales, B. Sartwell, The replacement of electroplating, *Surface and Coatings Technology*, Volume 81, Issue 1, May 1996, Pages 99-105, ISSN 0257-8972, [http://dx.doi.org/10.1016/0257-8972\(95\)02653-3](http://dx.doi.org/10.1016/0257-8972(95)02653-3).
19. Sadao Asanabe, Applications of ceramics for tribological components, *Materials & Design*, Volume 9, Issue 5, September–October 1988, Pages 253-262, ISSN 0261-3069, [http://dx.doi.org/10.1016/0261-3069\(88\)90002-7](http://dx.doi.org/10.1016/0261-3069(88)90002-7).
20. Bach, Friedrich-Wilhelm: *The Coatings in Manufacturing Engineering*, Stafa-Zuerich: Trans Tech, 2010. ISBN 9780878492725.
21. Martin, Peter M. *Handbook of Deposition Technologies for Films and Coatings*. Amsterdam: Elsevier, 2010. ISBN 9780815520313.
22. Fischer, Alfons, and Kirsten Bobzin. *Friction, Wear and Wear Protection*. Weinheim: Wiley, 2011. ISBN 9783527628520, <http://dx.doi.org/10.1002/9783527628513>.
23. Kerridge, M., and J. K. Lancaster. 'The Stages In A Process Of Severe Metallic Wear'. *Proceedings of the Royal Society A: Mathematical, Physical and Engineering Sciences* 236.1205 (1956): 250-264. <http://dx.doi.org/10.1098/rspa.1956.0133>.
24. Cocks, M. 'Interaction Of Sliding Metal Surfaces'. *Journal of Applied Physics*. Volume 33. Issue 7 (1962): 2152-2161. <http://dx.doi.org/10.1063/1.1728920>.
25. Morton Antler, Processes of metal transfer and wear, *Wear*, Volume 7, Issue 2, March–April 1964, Pages 181-203, ISSN 0043-1648, [http://dx.doi.org/10.1016/0043-1648\(64\)90053-5](http://dx.doi.org/10.1016/0043-1648(64)90053-5).